Immune function of LRRK2

Oun, Asmaa

DOI:
10.33612/diss.253651629

Chapter 5

The tale of proteolysis targeting chimeras (PROTACs) for Leucine-Rich Repeat Kinase 2 (LRRK2)

Markella Konstantinidou[+],[1] Asmaa Oun[+],[2] Pragya Pathak[+],[3] Bidong Zhang,[1] Zefeng Wang,[1] Frans ter Brake,[1] Amalia M. Dolga,[2] Arjan Kortholt,[3,4] and Alexander Dömling*[1]

[1] Department of Pharmacy, Group of Drug Design, University of Groningen, The Netherlands

[2] Department of Molecular Pharmacology, Groningen Research Institute of Pharmacy (GRIP), University of Groningen, The Netherlands

[3] Department of Cell Biochemistry, Groningen Institute of Biomolecular Sciences & Biotechnology,

University of Groningen, The Netherlands

[4] YETEM-Innovative Technologies Application and Research Centre Suleyman Demirel University, Isparta, Turkey

[+] These authors contributed equally to this work

* Corresponding author

ChemMedChem. 2021 Mar 18;16(6):959-965.
doi: 10.1002/cmdc.202000872

ABSTRACT

Here we present the rational design and synthetic methodologies towards proteolysis-targeting chimeras (PROTACs) for the recently-emerged target leucine-rich repeat kinase 2 (LRRK2). Two highly potent, selective, brain-penetrating kinase inhibitors were selected, and their structure was appropriately modified to assemble a cereblon-targeting PROTAC. Biological data show strong kinase inhibition and the ability of the synthesized compounds to enter the cells. However, data regarding the degradation of the target protein are inconclusive. The reasons for the inefficient degradation of the target are further discussed.

Keywords: cereblon · degradation · LRRK2 · Parkinson's disease · PROTAC

INTRODUCTION

Parkinson's disease (PD) is one of the most common neurodegenerative diseases and, although most PD cases are idiopathic and the etiology is largely unknown, both environmental and genetic factors are implicated. Leucine-rich repeat kinase 2 (*LRRK2*) encoded by PARK8 is among the implicated genes for PD. *LRRK2* mutations have been observed in a number of idiopathic late-onset PD or Parkinson's disease patients and are the most common cause of familial PD.[1–3] Importantly, recently it has been found that LRRK2 activity was enhanced in postmortem brain tissue from patients with idiopathic PD.[4] Therefore, LRRK2 is considered as an essential player in PD pathogenesis and targeting LRRK2 thus might be beneficial for PD in general.

LRRK2 is a large protein, consisting of 2527 amino acids and including multiple domains **(Figure 1)**. Interestingly, it contains both a kinase and a GTPase domain. Regarding the mutations, they mostly occur in the GTPase and the kinase domain, leading to increased kinase activity and autophosphorylation. A significant number of disease-associated LRRK2 mutations has been identified to date, among which five missense mutations (R1441C, R1441G, Y1699C, G2019S and I2020T) are linked to PD pathogenesis.[5,6] There have been extensive drug discovery efforts to develop inhibitors for LRRK2, focusing on ATP competitive active-site kinase inhibitors in particular.

Starting in 2006, three patent reviews have been published, covering the numerous potent scaffolds against the target.[7–9] In 2018, the first clinical trial (NCT03710707) was announced by Denali Therapeutics, followed by a second clinical trial in 2019 (NCT04056689).[10] The structures of DNL201 and DNL151 are not yet disclosed.

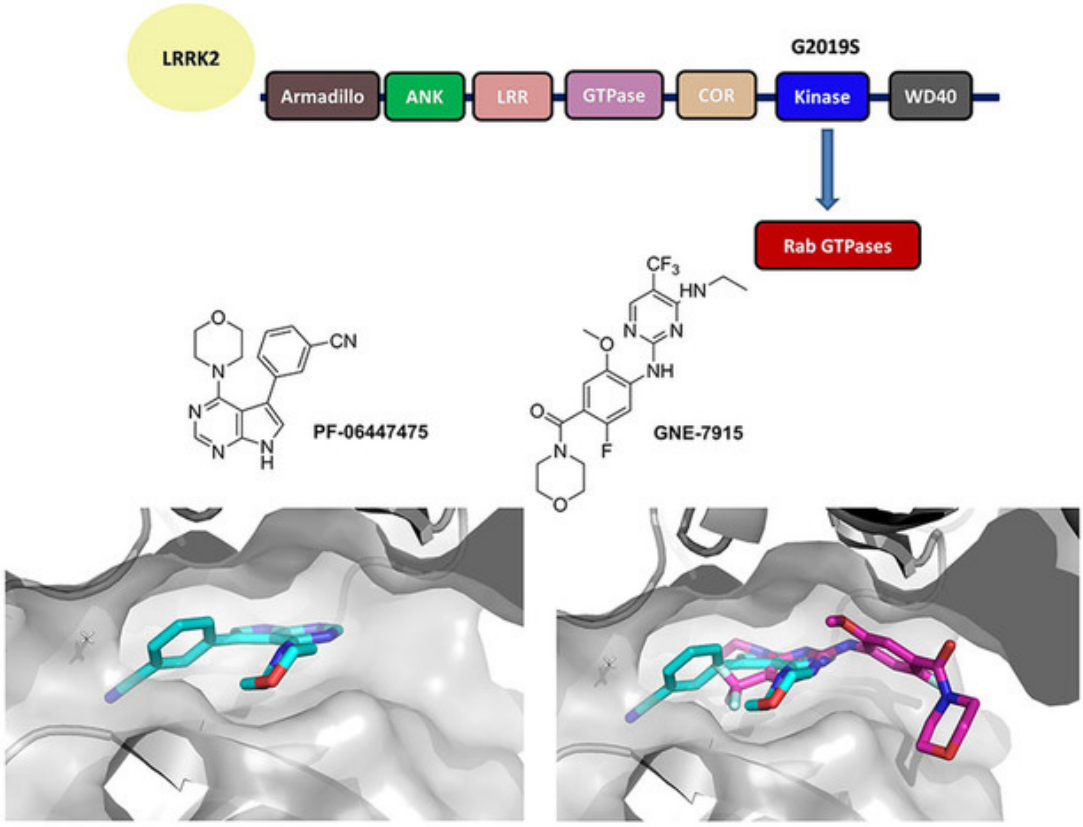

Figure 1: LRRK2, a PD target. **Top:** Functional LRRK2 moieties. **Middle:** 2D structures of two potent small molecules (PF-06447475, GNE-7915) inhibiting the LRKK2 kinase. **Below left:** the crystal structure of PF-06447475 (cyan sticks) with MST3 (grey surface; PDB ID: 4 U8Z), **below right:** overlap of a docking pose of GNE-7915 (magenta sticks) over PF-06447475 (cyan sticks) in MST3 active site (grey surface).

Here we explore the possibility of degrading LRRK2 using a proteolysis targeting chimera (PROTAC) strategy, instead of inhibiting its activity. PROTACs in the last few years have shown tremendous opportunities for modulating challenging or traditionally considered “undruggable” targets. Despite the fact that kinase inhibitors for LRRK2 have yet failed to reach the market, the potential of degrading LRRK2, as an alternative aim, has not been thoroughly investigated. In our approach, the starting points for designing and synthesizing PROTACs were known kinase inhibitors. Due to the abundance of scaffolds in the literature, the following requirements were considered significant in the choice of the inhibitors: 1) high potency, preferably low nanomolar inhibitors; 2) high selectivity in the kinome; 3) penetration of the blood - brain barrier; 4) availability of structural data regarding the binding mode; 5) solvent exposed functional group to attach the linker without compromising the kinase binding; 6) number of synthetic steps; 7) cost and availability of starting materials.

Based on those requirements, two scaffolds were selected: PF-06447475, developed by Pfizer and GNE-7915, developed by Genentech **(Figure 1)**. In particular PF-06447475, has an IC_{50} of 3 nM in the enzyme assay, 25 nM in the whole cell assay, is brain penetrant, highly selective in the kinome and does not show toxicity in rat models. The co-crystal structure with MST3 kinase is reported (PDB ID: 4U8Z).[11] GNE-7915 is also highly potent (K_i 2 nM in

the biochemical assay, IC_{50} 9 nM in the cellular assay), brain penetrant and with high kinome selectivity (1 out of 187).[12] In this case, only a docking pose with JAK2 is published; however, the described extensive SAR is sufficient to guide the structural modifications for a PROTAC.

In particular, the available structural data for PF-06447475 show that the oxygen of the morpholine participates in a hydrogen bond that is important for selectivity among the kinome, however, position 3 of the morpholine is solvent exposed and it could be used to attach a linker. On the contrary, for GNE-7915, the morpholine moiety seems to be completely solvent exposed and the hypothesis is that it is not a strict requirement for binding. In order to choose which E3 ligase to target, the expression levels in different tissues were checked in the database of Protein Atlas.[13] A comparative analysis revealed that cereblon and mouse double minute 2 homolog (MDM2) are expressed in the same parts of the brain, whereas Von Hippel Lindau (VHL) is not. MDM2 is expressed in all tissues in high levels, so to address possible selectivity issues cereblon seemed a better choice to begin with. The original routes for resynthesizing PF-06447475 and GNE-7915 were followed and then small modifications were considered in order to improve the yields of intermediates and thus facilitate the synthesis of PROTACs **(Scheme 1).**

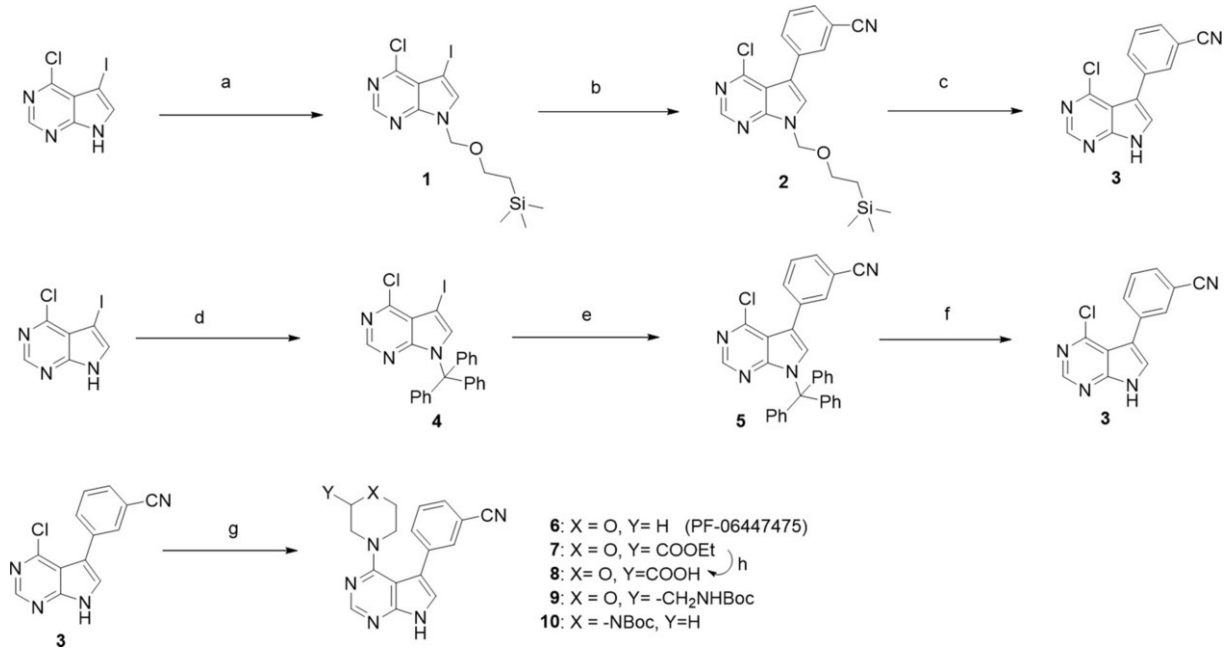

Scheme 1: Synthetic routes to reach main intermediate (**3**) for PF-06447475-based PROTACs; original (top), modified (middle). Bottom: transformations to intermediates with functional groups. *Reagents and conditions*: a) NaH, SEM-Cl, THF, 0 °C to RT, 3 h, 40 % yield; b) (3-cyanophenyl)boronic acid, 1 % $Pd(dppf)Cl_2$, K_2CO_3, DME/H_2O, reflux 3 h, 30 % yield; c) TFA, RT, 24 h, 60 % yield; d) trityl chloride, $CHCl_3$, Et_3N, RT, 1 h, quantitative; e) (3-cyanophenyl)boronic acid, 0.004 % $Pd(dppf)Cl_2$, $NaHCO_3$, toluene/EtOH, reflux 24 h, 60 % yield; f) TFA, CH_2Cl_2, RT, 24 h, 90 % yield; g) morpholine for (**6**) *tert*-butanol, DIPEA, reflux 3 h, or ethyl morpholine-2-carboxylate for (**7**) or *tert*-butyl *N*-(morpholin-2-ylmethyl)carbamate for (**9**) or *N*-Boc-piperazine for (**10**), EtOH, DIPEA, MW, 150 °C, 1 h, yields 26–30 %; h) LiOH, THF/H_2O, 65 % yield.

For PF-06447475, the main intermediate (**3**) was synthesized in three steps as shown in **scheme 1**. The original route[11,14] (top) led to intermediate (**3**) in only 8% overall yield and required two column purifications. However, by simply changing the protecting group in the first step from (2-chloromethoxyethyl) trimethylsilane (SEM-Cl) to trityl-chloride,[15] the yield became almost quantitative. Optimization of the Suzuki coupling also increased the yield significantly, and now the optimized route (middle route), led to intermediate (**3**) in 54% yield over three steps, requiring only one column purification.

After obtaining (**3**), the original inhibitor PF-06447475 (**6**) was synthesized with a nucleophilic aromatic substitution with morpholine. In order to attach suitable linkers for the PROTACs, morpholines substituted on position 3 were used, bearing either an ester group or a Boc-protected amine to obtain intermediates (**7**) and (**9**), respectively. Boc-piperazine was also used in a similar way for intermediate (**1**). The nucleophilic aromatic substitution was performed under microwave irradiation instead of reflux.

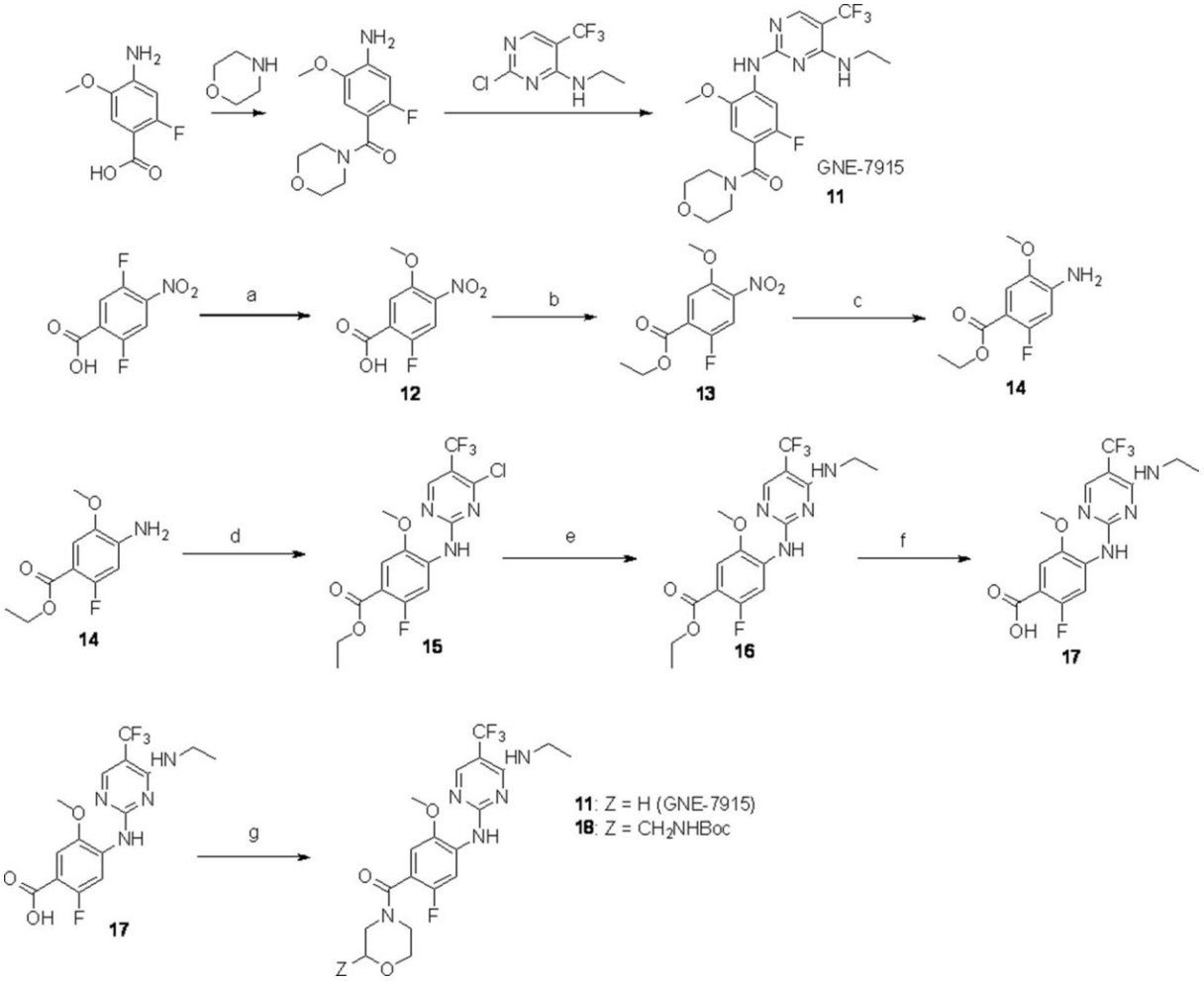

Scheme 2: Synthetic routes to GNE-7915: original (top), modified (middle) and intermediates for GNE-7915-based PROTACs (bottom). Reagents and conditions: a) MeOH, KOH, RT, 2 h, yield 92 %; b) EEDQ, EtOH, reflux 5 h, quantitative; c) stannous chloride, EtOH/H2O, reflux 4 h, quantitative; d) 2,4-dichloro-5-(trifluoromethyl) pyrimidine, zinc chloride, diethyl ether, CH2Cl2, tert-butanol, triethylamine, 0 °C to RT, 48 h, 40 % yield; e) ethanamine, triethylamine, THF, 0 °C to RT, 1 h, 88 % yield; f) LiOH, THF/H2O, 97 % yield; g) morpholine for (**11**) or tert-butyl N-(morpholin-2-ylmethyl)carbamate for (**18**), EEDQ, CHCl3, reflux 2 h, 40 % yield.

For GNE-7915 the original route[12] includes an amide coupling with morpholine and a nucleophilic aromatic substitution, with a starting material that also needs to be synthesized (**Scheme 2**, top). In GNE-7915 the morpholine part is solvent exposed and is also the position where the linkers can be attached. For the benefit of the overall route it is best to introduce the morpholine at the end of the synthesis. We developed an alternative route, starting from the commercially available 4-amino-2-fluoro-5-methoxybenzoic acid (**Scheme 2**, middle). The initial substitution of the fluorine with a methoxy group, was followed by an esterification and a reduction of the nitro group to obtain intermediate (**14**). The next step was a nucleophilic aromatic substitution using the bifunctional building block 2,4-dichloro-5-(trifluoromethyl)pyrimidine. Interestingly, the substitution can be performed selectively by using zinc chloride as catalyst.[16] The obtained intermediate (**15**) undergoes a substitution on the second chloride (**16**), followed by a hydrolysis to give the carboxylic acid (**17**), which is the key intermediate in this synthesis. Overall, the yield is 32% over 6 steps with only one column purification. The carboxylic acid (**17**) was used in an amide coupling reaction with morpholine to obtain GNE-7915 (**11**) and also in amide couplings directly with cereblon (CRBN) building blocks or with a substituted morpholine to obtain the amine intermediate (**18**).

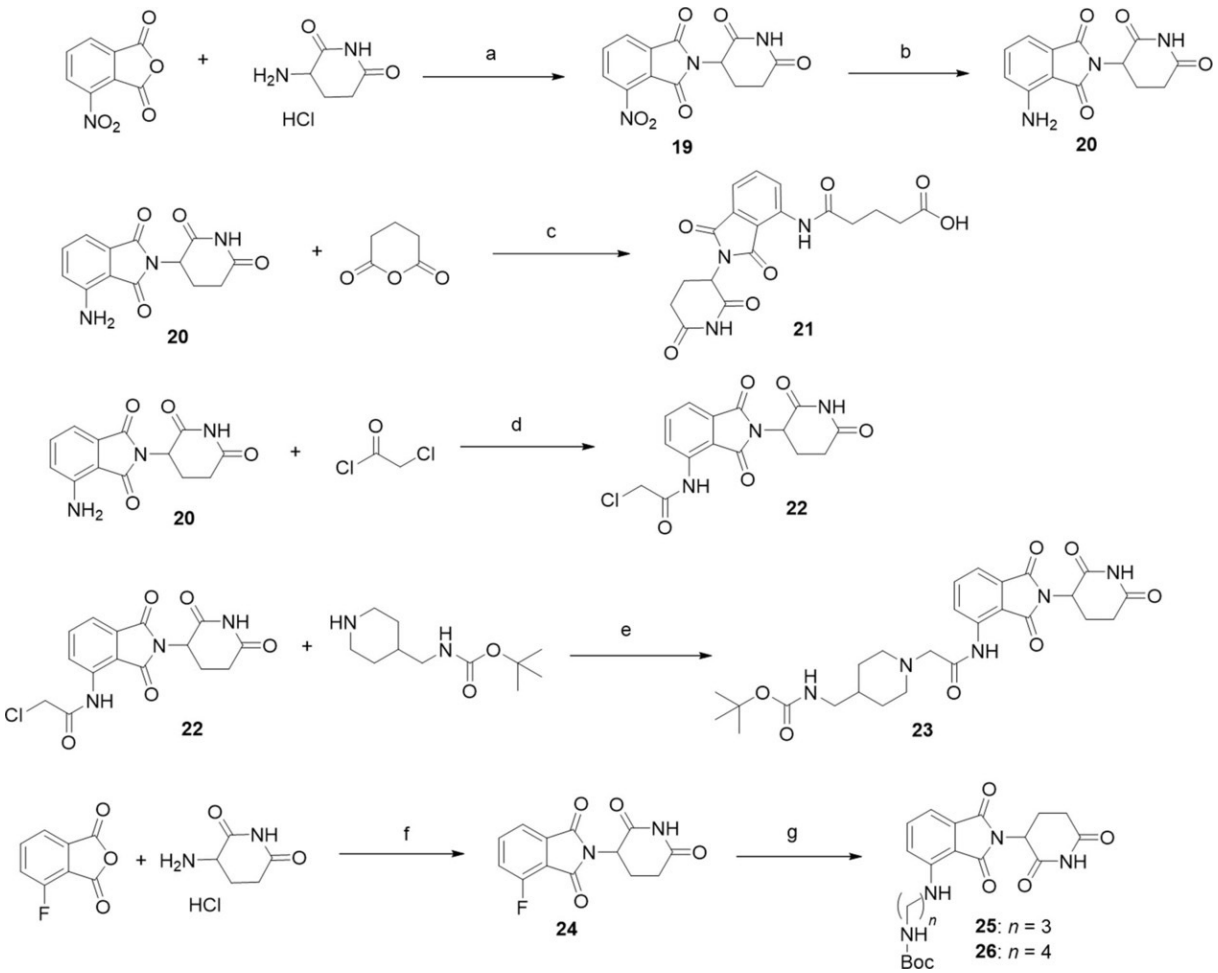

Scheme 3: Synthetic routes for CRBN-building blocks. Reagents and conditions: a) sodium acetate, acetic acid, overnight reflux, yield 90 %; b) H2, Pd/C, RT, 24 h, yield 92 %; c) potassium acetate, acetic acid, reflux 3 h, yield 32 %; d) THF, reflux, 30 min, yield 92 %; e) sodium iodide, potassium carbonate, THF, RT, yield 81 %; f) sodium acetate, acetic acid, overnight reflux, yield 85 %; g) N-Boc-propane-1,3-diamine or N-Boc-butane-1,4-diamine, DIPEA, DMF, overnight reflux, yield 60 %.

For the synthesis of cereblon building blocks two starting materials were used: the 4-nitroisobenzofuran-1,3-dione and the 4-fluoroisobenzofuran-1,3-dione (**Scheme 3**). The first synthetic step is the condensation of 4-nitroisobenzofuran-1,3-dione with 3-aminopiperidine-2,6-dione to obtain the nitro- substituted imide (**19**), which is then reduced to the aniline group to obtain pomalidomide (**20**). Pomalidomide was then used in an anhydride opening reaction obtain the carboxylic acid (**21**). Pomalidomide was also used in an acylation reaction with 2-chloroacetyl chloride to obtain the intermediate (**22**), which with a substitution reaction led to intermediate (**23**). In a similar way, the condensation of 4-fluoroisobenzofuran-1,3-dione with 3-aminopiperidine-2,6-dione was performed toobtain the fluoro-substituted imide (**24**), which underwent a nucleophilic aromatic substitution with linear Boc-protected diamines to obtain intermediates (**25**) and (**26**).

After synthesizing the appropriate kinase intermediates and the cereblon building blocks, the final PROTAC compounds were synthesized with amide coupling reactions. In all the cases of Boc-protected intermediates, the deprotection was performed with HCl in dioxane and the obtained salts were used directly in the amide coupling without purification. An overview of structures and coupling yields is shown in **Scheme 4**.

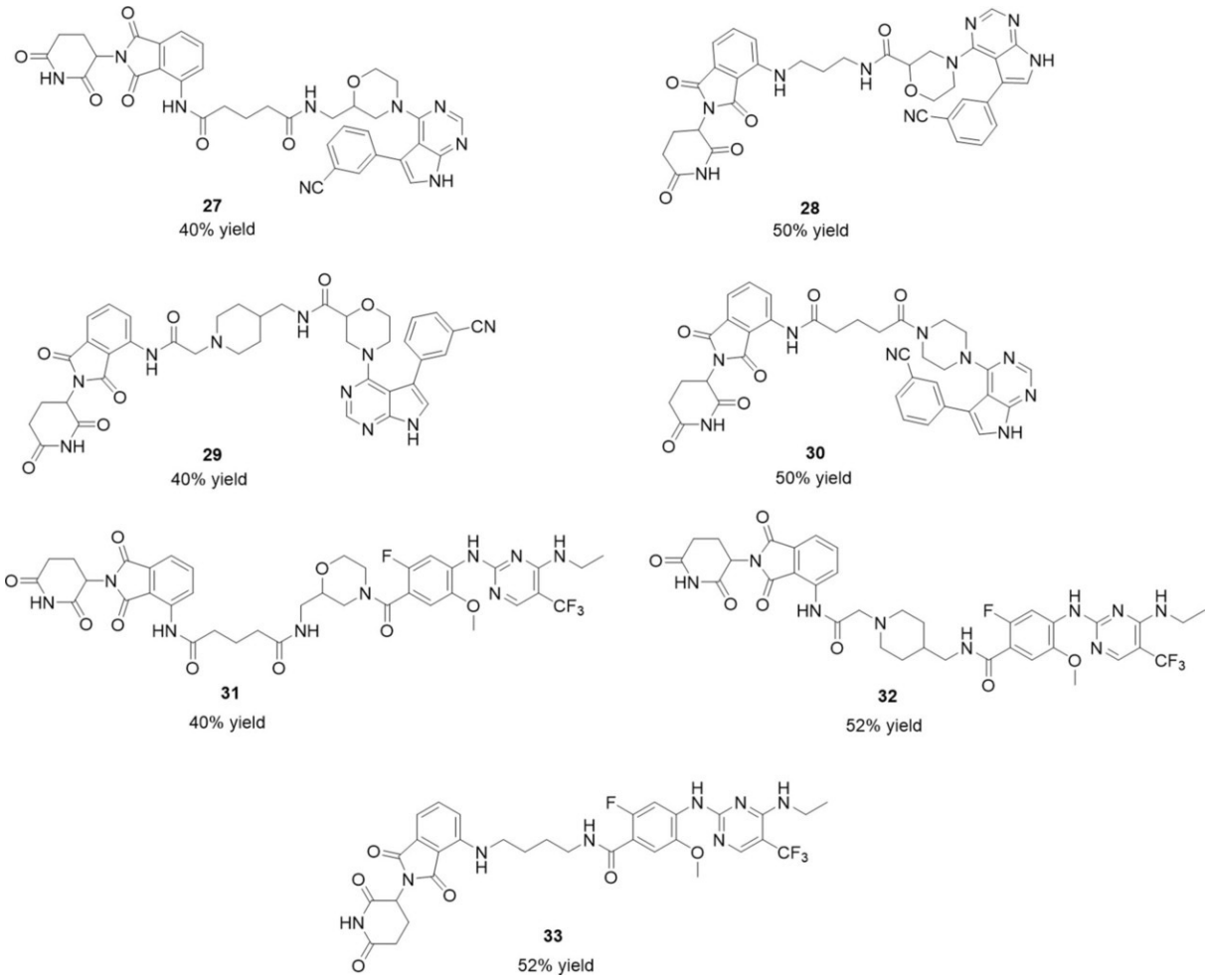

Scheme 4: Structures of PF-06447475-based-CRBN-PROTACs and GNE-7915-based-CRBN-PROTACs.

Then, the four PF-06447475/CRBN-based PROTACs and the three GNE-7915/CRBN-based PROTACs, as well as the original resynthesized inhibitors, were biologically evaluated. The original inhibitors were used as reference compounds. First, an in vitro kinase assay with the phosphorylation rate of a key LRRK2 autophosphorylation site (S1292-LRRK2) as readout, revealed that the compounds were indeed potent kinase inhibitors (**Figures S1** and **S2** in the Supporting Information).

Then, in order to test whether the PROTACs were cell permeable and able to bind to the kinase pocket of LRRK2, confocal microscopy was performed. It is known that incubation of LRRK2 with ATP competitive inhibitors results in relocalization of overexpressed GFP-tagged LRRK2 onto microtubules.[17–20] HEK cells transfected with GFP-tagged LRRK2 were incubated with different PROTACs along with the original kinase inhibitors and DMSO as controls. Formation of green filaments was observed after incubation with the original inhibitors and most of the PROTACs conferring the ability of the majority of the synthesized PROTACs to penetrate the cells and attach to the kinase pocket of LRRK2 (**Figure 2A**).

We next determined the ability of different PROTACs to degrade LRRK2 in LRRK2 parental RAW 264.7 cells. For the initial screening, the cells were incubated with 2 concentrations (1 and 10 μM) of PROTACs for 24, 48 and 72 hours. Data from western blotting did not show any significant changes in the LRRK2 protein levels between the PROTAC treated cells and cells treated with the original kinase inhibitors, indicating that PROTACs were not able to cause LRRK2 degradation (**Figures 2B** and **C**). Furthermore, ubiquitination assays showed that one of the most potent and cell permeable PROTACs, PROTAC (33) (IC_{50}= 14.69 ± 6.14 nM) was unable to increase the ubiquitin signal compared to the DMSO or original inhibitor compound (**11**) (IC_{50}=17.3 ± 6.76 nM) (**Figure 2D**).

Despite the fact that the synthesized PROTACs were able to enter the cells and bind to the target, there a few possible hypotheses explaining their inability to induce ubiquitination and degradation of LRRK2. It could be argued at this point that the number of synthesized PROTACs was limited and more variations on the linkers, including length, flexibility and attachment points, could be explored. However, as two different highly potent LRRK2 ligands failed to induce the degradation of the target, despite showing target engagement and cell permeability, there are also other possible explanations to consider. One plausible hypothesis, is that due to the observed re-localization of LRRK2 to the microtubules and formation of stable filaments, LRRK2 might not be accessible to the E3 ligase component to form a ternary LRRK2-PROTAC-E3 ligase complex. Moreover, since the full-length structure of LRRK2 is not known, the proximity of lysine residues suitable for ubiquitination degradation to the kinase site might not be optimal. To date, the full-length structure of LRRK2 is not solved. Recently, a high resolution cryo-EM structure of the catalytic half of LRRK2 including the RoC/GTPase, COR, kinase and WD40 domains was reported.[20] The structure revealed that the kinase and GTPase domains are in close proximity. Notably, in the absence of kinase inhibitors, the kinase was in an inactive/open conformation in the cryoEM structure, whereas data showed that the microtubule-associated LRRK2 had the kinase domain in a closed and potentially active conformation. Moreover, kinase inhibitors also had an effect on the kinase domain conformation and in particular, inhibitors that promoted LRRK2-microtubule binding favored the closed kinase conformation. The proposed model indicates the complexity of targeting LRRK2. Villa et al.,[21] using cryoEM and integrative modeling, revealed the structure of LRRK2 in situ and showed that the GTPase domain is closer to the microtubule interface, in contrast to the kinase domain which is exposed to the cytoplasm.

Another aspect to be taken into account, is the properties of LRRK2 inhibitors. Although numerous scaffolds have been reported, in most of the cases, there is lack of structural data and differences in selectivity. This seems to be affecting also the degradation potential of LRRK2 inhibitors. At the time of manuscript submission, a patent highlight indicated the degradation of LRRK2 and compared two types of inhibitors: the aminopyrimidine analogs and the indazole analogs.[22,23] In agreement with our observations, the aminopyrimidine analogs failed to degrade the target. On the other hand, the indazole analogs seemed to be able to reduce the levels of LRRK2. The data taken together with our results, show that

the selection of LRRK2 inhibitors is crucial for the development of degraders. Additionally, very recently, a high-throughput screen resulted in the discovery of a small molecule, which showed remarkable selectivity for G2019S-LRRK2, the most common LRRK2 pathogenic mutation.[24] This could be an interesting starting point for future studies of selective G2019S-LRRK2 degraders.

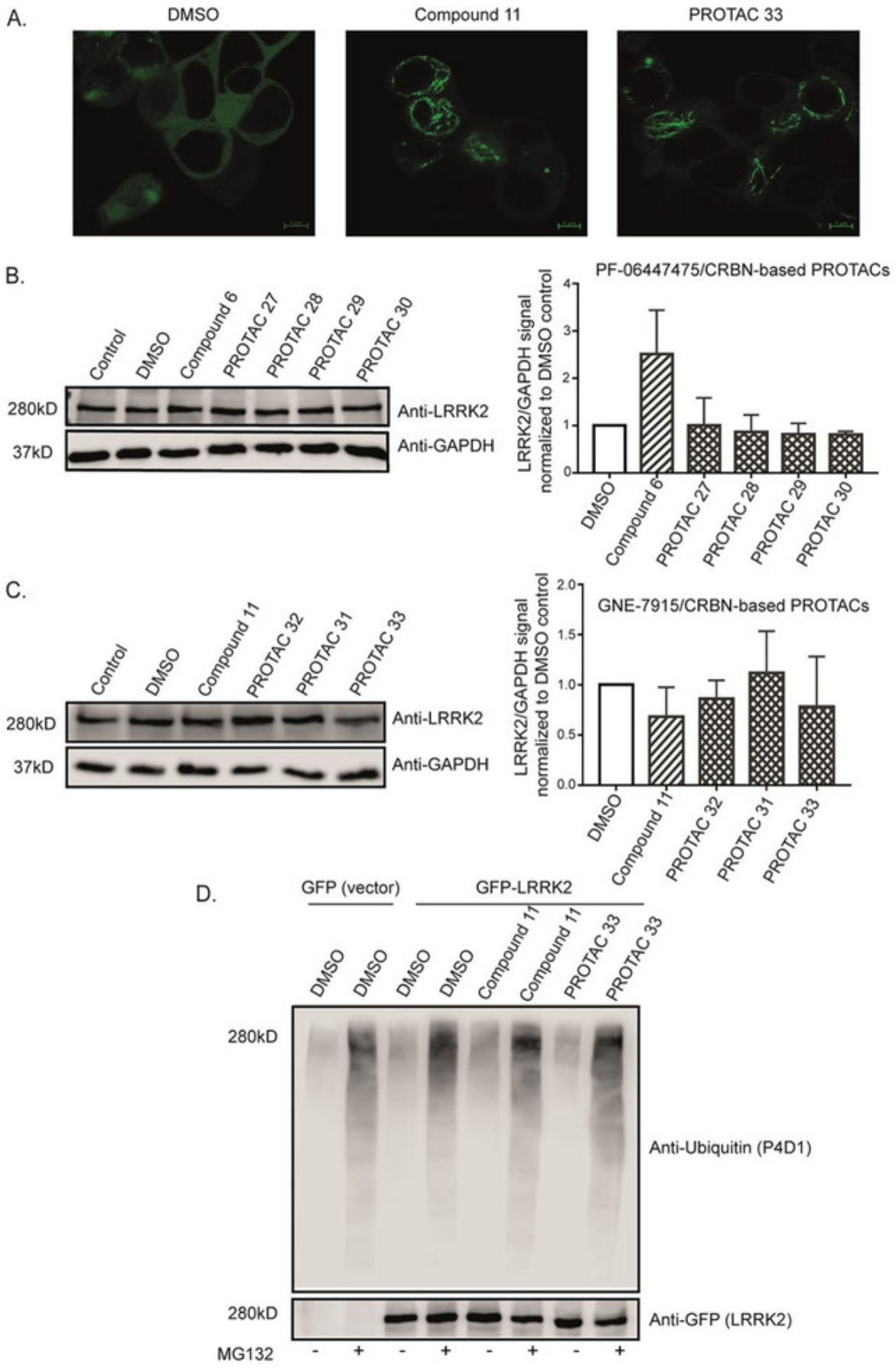
A.
DMSO
Compound 11
PROTAC 33
B.
Control
DMSO
Compound 6
PROTAC 27
PROTAC 28
PROTAC 29
PROTAC 30
280kD
37kD
Anti-LRRK2
Anti-GAPDH
PF-06447475/CRBN-based PROTACs
LRRK2/GAPDH signal normalized to DMSO control
C.
Control
DMSO
Compound 11
PROTAC 32
PROTAC 31
PROTAC 33
GNE-7915/CRBN-based PROTACs
D.
GFP (vector)
GFP-LRRK2
Anti-Ubiquitin (P4D1)
Anti-GFP (LRRK2)
MG132

Figure 2: PROTACs are cell-permeable yet not increasing LRRK2 degradation and ubiquitination. **A)** Confocal microscopy of GFP-tagged LRRK2-transfected HEK293 cells showing LRRK2 localization inside cells treated with DMSO, original kinase inhibitor and one of the PROTACs. The images show that the original kinase inhibitor and the PROTAC compound are cell-permeable and able to induce LRRK2 localization to the microtubules depicted as green filaments. **B)** and **C)** Representative western blots of LRRK2 parental RAW 264.7 cells treated with 10 μM of different PROTACs together with the original kinase inhibitors and DMSO controls for 24 h and immunoblotted with LRRK2 and GAPDH as a loading control. The quantification of the blots (n=3) shows that different PROTACs are not affecting LRRK2 degradation compared to the original kinase inhibitor.. **D)** GFP-tagged LRRK2 transfected HEK293 cells were treated with DMSO, original kinase inhibitor (**11**) and PROTAC (**33**) with or without MG132 for 24 h. An ubiquitin assay was performed on the collected cells. The samples were immunoblotted with anti-ubiquitin (P4D1) for the ubiquitin signal and anti-GFP for the LRRK2 signal. The blot shows that MG132 can enhance the ubiquitin signal and that neither the original kinase inhibitor (**11**) nor PROTAC (**33**) increase LRRK2 ubiquitination compared to the DMSO treated control.

To date, although PROTACs have been successful in challenging targets, the task of developing degraders is not trivial. Especially in the case of LRRK2, which remains an elusive drug target, a better understanding of its structure and conformational changes, as reported very recently, is necessary in order to further explore the possibility of degrading it and additionally to understand the reasons for the observed differences when highly potent LRRK2 inhibitors were modified into potential degraders. Overall, in this work, we aim to underline the challenges in degrading a target, for which the full structure is not yet known. We believe that future work will enable the rational development of a successful LRRK2-targeting PROTAC, following a more complete picture of LRRK2 structure and dynamics.

MATERIALS AND METHODS

- **General remarks**

Nuclear magnetic resonance spectra were recorded on a Bruker Avance 500 spectrometer (^{1}H-NMR at 500 MHz and ^{13}C-NMR at 126 MHz with tetramethylsilane (TMS) as internal standard). Chemical shifts for ^{1}H-NMR were reported as δ values and coupling constants were in hertz (Hz). The following abbreviations were used for spin multiplicity: s = singlet, b = broad singlet, d = doublet, t = triplet, q = quartet, dd = double of doublets, ddd = double of doublet of doublets, dt = doublet of triplets, td = triplet of doublets, m = multiplet. Chemical shifts for ^{13}C-NMR were reported in ppm relative to the solvent peak. Thin layer chromatography was performed on Fluka precoated silica gel plates (0.20 mm thick, particle size 25 μm). Flash chromatography was performed on a Teledyne ISCO Combiflash Rf, using RediSep Rf Normal-phase Silica Flash Columns (Silica Gel 60 Å, 230 - 400 mesh) and on a Reveleris® X2 Flash Chromatography, using Grace® Reveleris Silica flash cartridges (12 grams). Reagents were purchased from commercial suppliers (Sigma Aldrich, ABCR, Acros, AK Scientific, Combiblocks, Fluorochem) and used without any purification unless otherwise noted. Electrospray ionization mass spectra (ESI-MS) were recorded on a Waters Investigator Semi-prep 15 SFC-MS instrument. High resolution mass spectra were recorded using Orbitrap-Velos (Thermo) at a resolution of 60000@m/z400. Microwave reactions were carried out in a Biotage Initiator™ Microwave Synthesizer. The hydrogenation reaction was performed with a Parr Apparatus.

- **General experimental procedures**

Procedure A1 (Protecting step with SEM-Cl): in a 500ml round bottom flash 4-chloro-5-iodo-7Hpyrrolo[2,3-d]pyrimidine (17.9 mmol, 1 equiv) was dissolved in dry THF (120ml). Cooling in an ice bath and addition of NaH (19.69 mmol, 1.1 equiv) in portions as solid. The reaction mixture was stirred at 0°C for 1h and then (2-chloromethoxyethyl)trimethylsilane (SEM-Cl) (19.3 mmol, 1.08 equiv) was added dropwise. After the addition, the reaction mixture was allowed to reach rt. Stirring at rt for 4h. The reaction was quenched with saturated $NaHCO_3$ (120 ml). THF was removed under reduced pressure and the residue was extracted with EtOAc (100 ml x 3). The combined organic phases were dried over $MgSO_4$, filtered and the crude product was purified by column chromatography (PE – EtOAc, 0 – 20% EtOAc in PE).

Procedure A2 (Protecting step with trityl-Cl): in a round bottom flash 4-chloro-5-iodo-7Hpyrrolo[2,3-d]pyrimidine (17.9 mmol, 1 equiv) was suspended in dry $CHCl_3$ (45ml). Triethylamine was added (27 mmol, 1.5 equiv) and the suspension was cooled at 0°C. Trityl chloride (21.48 mmol, 1.2 equiv) was added in portions as solid. The reaction mixture was stirred at 0°C for 15 min under $CaCl_2$ tube and then at rt for 1h. Solvent was removed under reduced pressure. 100ml MeOH were added in the residue and the formed solid was filtered under reduced pressure and dried under vacuum.

Procedure B1 (Suzuki coupling on intermediate 1): in a 3-neck 500ml round bottom flask 4-chloro-5-iodo-7-((2-(trimethylsilyl)ethoxy)methyl)-7H-pyrrolo[2,3-d]pyrimidine (1) (7.1 mmol, 1equiv), (3-cyanophenyl)boronic acid (7.81 mmol, 1.1 equiv) and K_2CO_3 (21.3 mmol, 3 equiv) were dissolved in a mixture of DME – H_2O (4:1, 100ml). The reaction mixture was degassed for 15min and then $Pd(dppf)Cl_2$ (0.355mmol, 0.05 equiv) was added in one portion. The reaction mixture was heated at reflux for 3h, under N_2 flow. Then, it was allowed to reach rt and was diluted with saturated NaCl (100ml) and it was extracted with EtOAc (100ml x3). The combined organic phases were dried over MgSO4, filtered and the crude product was purified by column chromatography (PE – EtOAc, 0 – 20% EtOAc in PE).

Procedure B2 (Suzuki coupling on intermediate 4): In a 3-neck round bottom flask 4-chloro-5-iodo-7-trityl-7H-pyrrolo[2,3-d]pyrimidine **(4)** (9.6 mmol, 1 equiv) and (3-cyanophenyl) boronic acid (19.2 mmol, 2 equiv) were suspended in a 5:1 mixture toluene : EtOH (15 ml : 3 ml), followed by the addition of a saturated solution of $NaHCO_3$ (18ml). The reaction mixture was degassed for 15min and then $Pd(dppf)Cl_2$ (0.0384 mmol, 0.004 equiv) was added in one portion. The reaction mixture was heated overnight at 85°C under N_2 flow. The next day, the reaction mixture was allowed to reach rt, H_2O was added and the reaction mixture was extracted with EtOAc (x3). The combined organic phases were washed with 1N NaOH (x2), Brine (x3), dried over $MgSO_4$, filtered and the solvents were removed under reduced pressure. The crude product was purified by column chromatography (PE – EtOAc, 0 – 20% EtOAc in PE).

Procedure C1 (Deprotection of SEM-group): 3-(4-chloro-7-((2-(trimethylsilyl)ethoxy) methyl) -7Hpyrrolo[2,3-d]pyrimidin-5-yl)benzonitrile **(2)** (2 mmol, 1 equiv) was dissolved in 5ml TFA. Stirring rt overnight under $CaCl_2$ tube. DCM was added (10 ml) and the solvents were removed under reduced pressure to get a yellow oil. 15ml of methanol were added to get a yellow suspension. Under stirring at 0°C, solid K_2CO_3 was added in small portions until pH>12. Methanol was removed under reduced pressure and water was added (5ml). The suspension was filtered under vacuum and the obtained solid was washed with water and dried under vacuum.

Procedure C2 (Deprotection of trityl-group): 4-chloro-5-iodo-7-trityl-7H-pyrrolo[2,3-d] pyrimidine **(5)** (5.1mmol, 1 equiv) was dissolved in DCM (20ml). The solution was cooled in an ice-bath and TFA (10ml) was added. Stirring at 0°C for 10 min and then rt overnight under $CaCl_2$ tube. Solvents were removed under reduced pressure. The oily residue was dissolved in 20ml MeOH. Under stirring at 0°C, solid K_2CO_3 was added in small portions until pH>12. Methanol was removed under reduced pressure and water was added (5ml). The suspension was filtered under vacuum and the obtained solid was washed with water and dried under vacuum. The obtained solid was triturated with diethylether to remove impurities.

Procedure D1 (Nucleophilic aromatic substitution with morpholine): 3-(4-chloro-7H-pyrrolo[2,3-d]pyrimidin-5-yl)benzonitrile **(3)** (0.39 mmol, 1 equiv) was suspended in *tert*-butanol (5 ml). DIPEA (0.78 mmol, 2 equiv) and morpholine (0.43 mmol, 1.1 equiv) were added and the reaction mixture was heated at reflux for 3h. Solvent was removed and the crude was purified by column chromatography (DCM – MeOH, 0 – 6% MeOH in DCM).

Procedure D2 (Nucleophilic aromatic substitution with 3-substituted morpholines or Bocpiperazine): in a microwave vial 3-(4-chloro-7H-pyrrolo[2,3-d]pyrimidin-5-yl)benzonitrile **(3)** (0.39 mmol, 1 equiv) was suspended in ethanol (2 ml). DIPEA (0.78 mmol, 2 equiv) and the appropriate secondary amine (0.43 mmol, 1.1 equiv) were added and the reaction mixture was subjected to microwave irradiation (1h, 150°C). Solvent was removed and the crude was purified by column chromatography (DCM – MeOH, 0 – 6% MeOH in DCM).

Procedure E (Ester hydrolysis): the ethyl ester (1equiv) was suspended in a mixture of THF – H_2O (2:1, 0.2M) and LiOH (2 equiv) was added. The reaction mixture was stirred rt overnight. Solvents were removed under reduced pressure and the residue was dissolved in 5ml H_2O. Cooling at 0°C and acidification with 2N HCl until pH = 1. Extraction with EtOAc (50 ml x3), drying over $MgSO_4$, filtration and evaporation under reduced pressure.

Procedure F (Substitution of fluorine with methoxy group): In a round bottom flask, 2,5-difluoro-4-nitrobenzoic acid (24.6 mmol, 1 equiv) was dissolved in methanol (80 ml) at room temperature. A solution of freshly prepared KOH (73.8 mmol, 3 equiv) in 30 ml MeOH was added dropwise over 20 min. The formed suspension was stirred at room temperature for 2 h and eventually the reaction mixture became a yellow solution. Methanol was removed under reduced pressure and the residue was suspended in 50 ml of EtOAc. While cooling in an ice-bath acidification with 2N aqueous HCl, until pH =1 and extraction with EtOAc (80 ml

x3), drying over $MgSO_4$, filtration and evaporation under reduced pressure.

Procedure G (Esterification): 2-fluoro-5-methoxy-4-nitrobenzoic acid **(12)** (9.3 mmol, 1 equiv) was dissolved in ethanol under stirring. N-Ethoxycarbonyl-2-ethoxy-1,2-dihydroquinoline (EEDQ, 11.2 mmol, 1.2 equiv) was added in portions. The reaction mixture was heated at reflux for 5 h. Solvent was removed under reduced pressure and the residue was dissolved in EtOAc (100 ml) and washed with 1N HCl (x2), H2O (x2) and Brine (x2). The organic phase was dried over MgSO4, filtered and the solvent was removed under reduced pressure.

Procedure H (Reduction with stannous chloride): ethyl 2-fluoro-5-methoxy-4-nitrobenzoate **(13)** (9.1 mmol, 1 equiv) was suspended in a mixture of ethanol – water (65 ml : 6.5 ml). Stannous chloride (36.4 mmol, 4 equiv) was added in portions at room temperature. The reaction mixture was heated at reflux for 4h. Solvent was removed under reduced pressure and the residue was diluted with 50 ml EtOAc. Under stirring, saturated $NaHCO_3$ was added until pH=8. Extraction with EtOAc (80 ml x3). The combined organic phases were dried over $MgSO_4$, then passed through a pad of celite and the solvent was removed under reduced pressure.

Procedure I (Selective nucleophilic aromatic substitution of chlorine): ethyl 4-amino-2-fluoro-5-methoxybenzoate **(14)** (9.0 mmol, 1 equiv) was dissolved in a mixture of diethylether (6.0 ml), *tert*butanol (4.0 ml) and DCM (15 ml) and was then cooled in an ice-bath. At 0°C under stirring, zinc chloride (18.0 mmol, 2 equiv) was added in portions as solid, followed by the addition of 2,4-dichloro-5-(trifluoromethyl)pyrimidine (9.0 mmol, 1.0 equiv) and triethylamine (9.9 mmol, 1.1 equiv). The reaction mixture was stirred at 0°C for 1h under $CaCl_2$ tube and then at room temperature for 48h. The reaction was monitored by TLC (PE: EtOAc 8:2). The reaction mixture was diluted with 40 ml DCM and slowly 40 ml of water were added (bubbling was observed). Stirring rt for 15 min and then extraction with DCM (50 ml x3). The combined organic phases were washed with Brine, dried over $MgSO_4$, filtered and the solvent was removed under reduced pressure. The crude residue was purified by column chromatography PE: EtOAc (0-50% EtOAc in PE).

Procedure J (Nucleophilic aromatic substitution of chlorine): ethyl 4-((4-chloro-5-(trifluoromethyl)pyrimidin-2-yl)amino)-2-fluoro-5-methoxybenzoate **(15)** (3.3 mmol, 1 equiv) was dissolved in 15 ml dry THF. Cooling at 0°C and then dropwise addition of a 2N solution of ethanamine (6.6 mmol, 2.2 equiv) under N2 flow. The reaction mixture was stirred at 0°C for 30 min and then rt for 2 h. Solvent was removed under reduced pressure. The residue was diluted with EtOAc (50ml) and washed with H_2O (x2) and Brine (x2). The organic phase was dried over $MgSO_4$, filtered and the solvent was removed under reduced pressure.

Procedure K (Synthesis of substituted 2-(2,6-dioxopiperidin-3-yl)isoindoline-1,3-diones): In a round bottom flask, the appropriate 4-substituted-isobenzofuran-1,3-dione (1 equiv), 3-aminopiperidine-2,6-dione hydrochloride (1 equiv) and sodium acetate (1.2 equiv) were mixed in AcOH (20 ml for 5 mmol scale). The resulting mixture was heated at 120°C

overnight. After cooling to room temperature, most of the AcOH was removed under reduced pressure and the residue was dissolved in the water, filtered and washed with water and dried with vacuum to obtain the crude compound.

Procedure L (Reduction): To a solution of 2-(2,6-dioxopiperidin-3-yl)-4-nitroisoindoline-1,3-dione (8 mmol, 1.0 equiv) in dry DMF (50 ml) was added the Pd/C (1.6mmol, 0.2 equiv) under N_2. The reaction mixture was hydrogenated with 3.0 atm H2 pressure at room temperature for 4 h (Parr Apparatus). The progress of the reaction was monitored by TLC. The reaction mixture was filtered over a pad of celite. The filtrate was diluted with EtOAc and the organic phase was washed with H_2O and Brine (x3), dried over $MgSO_4$ and filtered. The solvent was removed under reduced pressure, to obtain a solid, which was used directly in the next step.

Procedure M (Anhydride opening): A mixture of 4-amino-2-(2,6-dioxopiperidin-3-yl) isoindoline-1,3- dione (7.3 mmol, 1.0 equiv), potassium acetate (29.3 mmol, 4.0 equiv) and glutaric anhydride (29.23 mmol, 4.0 equiv) in glacial AcOH (60 ml) was heated at reflux under nitrogen for 3h. After cooling at room temperature, acetic acid was removed under reduced pressure and the residue was extracted with (EtOAc – H_2O). The organic phases were dried with $MgSO_4$, filtered and solvents were removed under reduced pressure. The crude product was purified by column chromatography (DCM – MeOH, 0 – 10% MeOH in DCM).

Procedure N (Amidation): To a stirred suspension of 4-amino-2-(2,6-dioxo(3-piperidyl)) isoindoline-1,3-dione (5.00 mmol, 1 equiv) in THF (30 ml), chloroacetyl chloride (5.5 mmol, 1.1 equiv) was added. The mixture was heated to reflux for 30 minutes. The solvent was evaporated under reduced pressure and the obtained solid was treated with diethyl ether (20 ml) and filtered to give the product, which was used directly in the next step.

Procedure O (Aliphatic substitution): A mixture of 2-chloro-*N*-(2-(2,6-dioxopiperidin-3-yl)-1,3-dioxoisoindolin-4-yl)acetamide (3.44 mmol, 1.0 equiv), *tert*-butyl (piperidin-4-ylmethyl) carbamate (3.8 mmol, 1.1 equiv), NaI (3.44 mmol, 1.0 equiv) and K_2CO_3 (6.88 mmol, 2 equiv) in THF (30 ml) was stirred at room temperature overnight. The solvent was removed under reduced pressure, water (50 ml) was added, and the reaction mixture was extracted with EtOAc (3 × 100 ml). The combined organic phases were washed with brine (50 ml), dried over MgSO4, filtered, and concentrated under reduced pressure. The crude product was purified by column chromatography (DCM: MeOH = 20:1).

Procedure P (Nucleophilic aromatic substitution of fluorine): The appropriate mono-Boc protected diamine (1.13 mmol, 1.1 equiv) was added to a stirred solution of 2-(2,6-dioxopiperidin-3-yl)-4- fluoroisoindoline-1,3-dione (1.03 mmol, 1.0 equiv) in DMF (1 M) and DIPEA (2.06 mmol, 2.0 equiv). The reaction mixture was stirred at 90°C for 12 h. Then the mixture was cooled to room temperature, poured into H_2O, and extracted twice with EtOAc (3 x 50 ml). The combined organic layers were washed with brine, dried over anhydrous Na_2SO_4 and filtered. Solvents were removed under reduced pressure and the crude product was purified by column chromatography (PE – EtOAc, 0 - 50% EtOAc in PE).

Procedure Q1 (Amide coupling with boc-protected amines): The appropriate boc-protected amine (1 equiv) was deprotected with 4N HCl in dioxane with stirring rt overnight. The reaction mixture was dried under vacuum. Diethylether was added (x2) and was removed under reduced pressure. The obtained HCl salt was used directly in the amide coupling. The HCl salt (1 equiv) was suspended in $CHCl_3$ (0.1M). Under stirring DIPEA (2 equiv) was added, followed by the addition of the carboxylic acid (1 equiv) and EEDQ (2 equiv). The reaction mixture was heated at reflux for 2h. Then it was allowed to reach rt and was purified directly by column chromatography (DCM – MeOH, 0 – 10% MeOH in DCM).

Procedure Q2 (Amide coupling with secondary amines): the carboxylic acid (1 equiv) and EEDQ (2 equiv) were stirred at rt in $CHCl_3$ (0.1M), followed by the addition of the secondary amine (1 equiv). The reaction mixture was heated at reflux for 2h. Then it was allowed to reach rt and was purified directly by column chromatography (DCM – MeOH, 0 – 10% MeOH in DCM).

5

- **Characterization data**

4-chloro-5-iodo-7-((2-(trimethylsilyl)ethoxy)methyl)-7H-pyrrolo[2,3-d]pyrimidine (1)

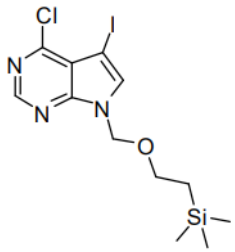

Obtained using procedure A1 on 17.9 mmol scale; 2.9 g, 7.1 mmol, yield 40%, white solid. ^{1}H NMR (500 MHz, DMSO-*d*6) δ 8.69 (s, 1H), 8.14 (s, 1H), 5.60 (s, 2H), 3.51 (t, *J* = 8.0 Hz, 2H), 0.82 (t, *J* = 8.0 Hz, 2H), -0.10 (s, 9H). ^{1}H NMR is in good agreement with published data. [s1]

3-(4-chloro-7-((2-(trimethylsilyl)ethoxy)methyl)-7H-pyrrolo[2,3-d]pyrimidin-5-yl) benzonitrile (2)

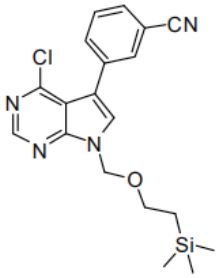

Obtained using procedure B1 on 7.1 mmol scale; 800 mg, 2.1 mmol, yield 30%, offwhite solid. ^{1}H NMR (500 MHz, DMSO-*d*6) δ 8.75 (s, 1H), 8.13 (s, 1H), 8.01 (b, 1H),7.90 – 7.86 (m, 2H), 7.72 – 7.66 (m, 1H), 5.70 (s, 2H), 3.59 (t, *J* = 8.0 Hz, 2H), 0.86 (t, *J* = 8.0 Hz, 2H), -0.08 (s, 9H). ^{1}H NMR is in good agreement with published data.[s1]

3-(4-chloro-7H-pyrrolo[2,3-d]pyrimidin-5-yl)benzonitrile (3)

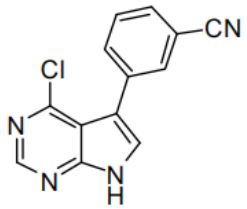

Obtained using procedure C1 on 2.0 mmol scale; 305 mg, 1.2 mmol, yield 60%, white solid. Obtained also using procedure C2 on 5.1 mmol scale; 1.2 g, 4.6 mmol, yield 90%, white solid. ^{1}H NMR (500 MHz, DMSO-*d*6) δ 8.48 (s, 1H), 7.94 (s, 1H), 7.87 – 7.85 (m, 2H), 7.71 (d, *J* = 7.9 Hz, 1H), 7.60 (t, *J* = 7.8 Hz, 1H).^{1}H NMR is in good agreement with published data.[s1] HRMS (ESI): m/z calcd for $C_{13}H_8N_4Cl$ $[M+H]^+$: 255.0432; found 255.0432.

4-chloro-5-iodo-7-trityl-7H-pyrrolo[2,3-d]pyrimidine (4)

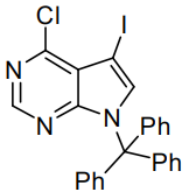

Obtained using procedure A2 on 17.9 mmol scale; 9.3 g, 17.85 mmol, yield 99%, white solid. ^{1}H NMR (500 MHz, $CDCl_3$) δ 8.27 (s, 1H), 7.38 (s, 1H), 7.31– 7.28 (m, 10H), 7.13 – 7.11 (m, 5H).^{1}H NMR is in good agreement with published data.[s2] HRMS (ESI): m/z calcd for $C_{25}H_{18}N_3Cl$ $[M+H]^+$: 522.0228; found 522.0227.

4-chloro-5-iodo-7-trityl-7H-pyrrolo[2,3-d]pyrimidine (5)

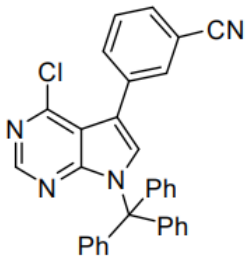

Obtained using procedure B2 on 9.6 mmol scale; 2.8 g, 5.7 mmol, yield 60%, white solid. ^{1}H NMR (500 MHz, $CDCl_3$) δ 8.35 (s, 1H), 7.77 – 7.74 (m, 2H), 7.66 – 7.63 (m, 1H), 7.51 (t, *J* = 7.8 Hz, 1H), 7.34 – 7.30 (m, 10H), 7.20 – 7.18 (m, 6H). ^{13}C NMR (126 MHz, $CDCl_3$) δ 152.7, 152.0, 150.0, 141.6, 134.9, 134.2, 133.5, 131.8, 131.4, 130.8, 130.6, 130.0, 129.8, 129.7, 128.7, 128.0, 127.8, 118.6, 116.1, 113.8, 112.2, 76.8.HRMS (ESI): m/z calcd for C_{32} H_{22} N_4 Cl $[M+H]^+$:497.1528; found 497.1525.

3-(4-morpholino-7H-pyrrolo[2,3-d]pyrimidin-5-yl)benzonitrile (6) [PF-06447475]

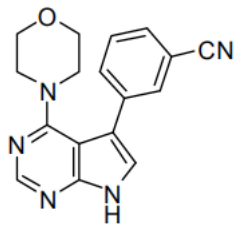

Obtained using procedure D1 on 0.39 mmol scale; 32 mg, 0.10 mmol, yield 26%, white solid. ^{1}H NMR (500 MHz, $CDCl_3$) δ 10.54 (s, 1H), 8.54 (s, 1H), 7.86 (s, 1H), 7.78 (d, *J* = 7.7 Hz, 1H), 7.62 (d, *J* = 7.7 Hz, 1H), 7.57 (t, *J* = 7.7 Hz, 1H), 7.28 (b, 1H), 3.56 – 3.54 (m, 4H), 3.32 – 3.30 (m, 4H).HRMS (ESI): m/z calcd for $C_{17}H_{16}ON_5$ $[M+H]^+$: 306.1349; found 306.1344.

ethyl 4-(5-(3-cyanophenyl) -7H-pyrrolo[2,3-d]pyrimidin-4-yl) morpholine-2-carboxylate (7)

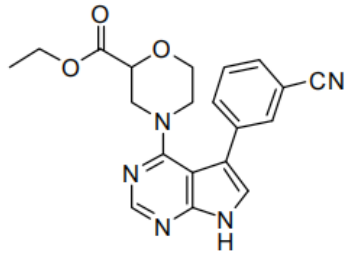

Obtained using procedure D2 on 0.39 mmol scale; 45 mg, 0.12 mmol, yield 30%, colorless oil. ^{1}H NMR (500 MHz, $CDCl_3$) δ 11.79 (s, 1H), 8.56 (s, 1H), 7.85 - 7.84 (m, 1H), 7.79 – 7.77 (m, 1H), 7.63 – 7.62 (m, 1H), 7.58 (d, *J* = 7.7 Hz, 1H), 7.36 (b, 1H), 4.16 (q, *J* = 7.1 Hz, 2H), 4.04 (dd, *J* = 9.9, 2.8 Hz, 1H), 3.97 – 3.95 (m, 1H), 3.89 (dd, *J* = 8.9, 2.7 Hz, 1H), 3.59 – 3.56 (m, 1H), 3.50 (td, *J* = 11.3, 2.4 Hz, 1H), 3.08 – 3.02 (m, 2H), 1.24 (t, *J* = 7.1 Hz, 3H). HRMS (ESI): m/z calcd for $C_{20}H_{20}O_3N_5$ $[M+H]^+$:378.1561; found 378.1555.

4-(5-(3-cyanophenyl)-7H-pyrrolo[2,3-d]pyrimidin-4-yl)morpholine-2-carboxylic acid (8)

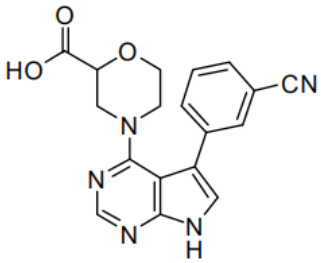

Obtained using procedure E on 0.12 mmol scale; 30 mg, 0.08 mmol, yield 65%, yellow solid.^{1}H NMR (500 MHz, DMSO-*d*6) δ 12.37 (s, 1H), 8.42 (s, 1H), 8.01 (b, 1H), 7.83 (d, *J* = 7.8 Hz, 1H), 7.76 (d, *J* = 7.7 Hz, 1H), 7.72 - 7.71 (m, 1H), 7.66 (t, *J* = 7.8 Hz, 1H), 4.02 – 4.00 (m, 1H), 3.73 – 3.71 (m, 2H), 3.04 – 2.99 (m, 2H), 2.87 – 2.84 (m, 2H). HRMS (ESI): m/z calcd for $C_{18}H_{16}O_3N_5$ $[M+H]^+$:350.1248; found 350.1244.

***tert*-butyl((4-(5-(3-cyanophenyl)-7H-pyrrolo[2,3-d]pyrimidin-4-yl)morpholin-2-yl) methyl)**

carbamate (9)

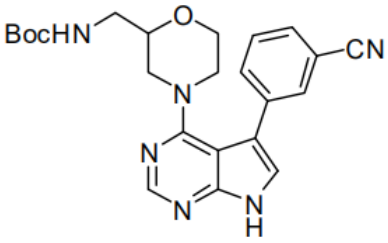

Obtained using procedure D2 on 0.39 mmol scale; 52 mg, 0.12 mmol, yield 30%, yellow solid.^{1}H NMR (500 MHz, $CDCl_3$) δ 12.24 (s, 1H), 8.52 (s, 1H), 7.82 (s, 1H), 7.77 (d, *J* = 7.6 Hz, 1H), 7.60 (d, *J* = 7.7 Hz, 1H), 7.56 (t, *J* = 7.7 Hz, 1H), 7.34 (b, 1H), 4.81 (b, 1H), 3.72 – 3.69 (m, 2H), 3.61 – 3.59 (m, 1H), 3.47 – 3.42 (m, 2H), 3.17 – 3.15 (m, 1H), 2.94 – 2.90 (m, 2H), 2.71 – 2.68 (m, 1H), 1.43 (s, 9H).^{13}C NMR (126 MHz, MeOD-*d4*) δ 161.7, 158.2, 154.2, 151.6, 138.0, 134.0, 132.9, 130.9, 124.4, 119.8, 116.2, 113.7, 104.4, 80.2, 75.6, 67.0, 53.4, 50.4, 43.6, 28.8. HRMS (ESI): m/z calcd for $C_{23}H_{27}O_3N_6$ $[M+H]^+$:435.2139; found 435.2135.

tert-butyl4-(5-(3-cyanophenyl)-7H-pyrrolo[2,3-d]pyrimidin-4-yl)piperazine-1-carboxylate (10)

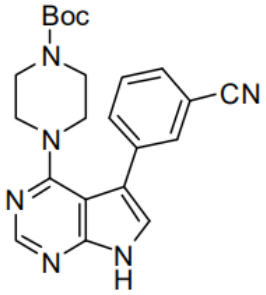

Obtained using procedure D2 on 2 mmol scale; 240 mg, 0.6 mmol, yield 30%, white solid.^{1}H NMR (500 MHz, $CDCl_3$) δ 11.04 (s, 1H), 8.52 (s, 1H), 7.84 (s, 1H), 7.77 (d, *J* = 7.7 Hz, 1H), 7.62 (d, *J* = 7.6 Hz, 1H), 7.56 (t, *J* = 7.7 Hz, 1H), 7.30 (s, 1H), 3.27 (b, 8H), 1.43 (s, 9H).^{13}C NMR (126 MHz, $CDCl_3$) δ 160.3, 154.5, 153.5, 150.9, 136.5, 132.5, 131.7, 130.1, 129.5, 121.8, 118.7, 115.3, 112.8, 103.2, 80.1, 49.5, 43.3, 28.4.

(4-((4-(ethylamino)-5-(trifluoromethyl)pyrimidin-2-yl)amino)-2-fluoro-5-methoxyphenyl)(morpholino)methanone (11) [GNE-7915]

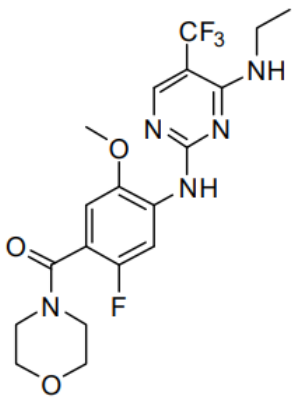

Obtained using procedure Q2 on 0.26 mmol scale; 46 mg, 0.103 mmol, yield 40%, white solid. ^{1}H NMR (500 MHz, $CDCl_3$) δ 8.44 (d, *J* = 12.3 Hz, 1H), 8.19 (s, 1H), 7.85 (s, 1H), 6.91 (d, *J* = 5.9 Hz, 1H), 5.22 (b, 1H), 3.91 (s, 3H), 3.80 – 3.77 (m, 4H), 3.68 – 3.66 (m, 2H), 3.62 – 3.59 (m, 2H), 3.45 – 3.43 (m, 2H), 1.32 (t, *J* = 7.2 Hz, 3H). ^{1}H NMR is in good agreement with published data.[s3] ^{13}C NMR (126 MHz, $CDCl_3$) δ 165.5, 160.3, 158.8, 154.4 (d, *J*=5.0 Hz), 152.3 (d, *J* =238.5 Hz), 144.1, 131.8 (d, *J* =12.3 Hz), 124.7 (q, *J* =270.3 Hz), 114.4 (d, *J* =19.2 Hz), 109.7 (d, *J* =5.0 Hz), 105.6 (d, *J* =31.8 Hz), 99.7, 66.8, 56.2, 47.7, 42.7, 36.4, 14.4. HRMS (ESI): m/z calcd for $C_{19}H_{22}O_3N_5F_4$ $[M+H]^+$:444.1653; found 444.165.

2-fluoro-5-methoxy-4-nitrobenzoic acid (12)

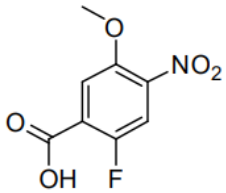

Obtained using procedure F on 24.6 mmol scale; 4.87 g, 22.6 mmol, yield 92%, light yellow solid. ^{1}H NMR (500 MHz, $CDCl_3$) δ 7.72 (d, *J* = 5.5 Hz, 1H), 7.66 (d, *J* = 9.2 Hz, 1H), 4.02 (s, 3H). ^{13}C NMR (126 MHz, $CDCl_3$) δ 167.2 (d, *J* = 3.8 Hz), 155.0 (d, *J* = 260.3 Hz), 148.4 (d, *J* = 3.2 Hz), 142.5 (d, *J* = 7.3 Hz), 121.6 (d, *J* = 11.1 Hz), 116.9, 114.6 (d, *J* = 28.7 Hz), 57.2.

ethyl 2-fluoro-5-methoxy-4-nitrobenzoate (13)

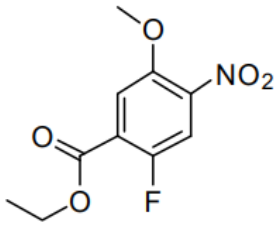

Obtained using procedure G on 9.3 mmol scale; 2.2 g, 9.1 mmol, yield 98%, offwhite solid. ^{1}H NMR (500 MHz, $CDCl_3$) δ 7.64 – 7.62 (m, 2H), 4.44 (q, *J* = 7.1 Hz, 2H), 3.99 (s, 3H), 1.42 (t, *J* = 7.1 Hz, 3H). ^{13}C NMR (126 MHz, $CDCl_3$) δ 162.9 (d, *J* = 4.3 Hz), 154.2 (d, *J* = 257.5 Hz), 148.4 (d, *J* = 3.0 Hz), 141.5 (d, *J* = 8.1 Hz), 123.51 (d, *J* = 12.0 Hz), 116.5, 114.4 (d, *J* = 29.0 Hz), 62.3, 57.1, 14.1.

ethyl 4-amino-2-fluoro-5-methoxybenzoate (14)

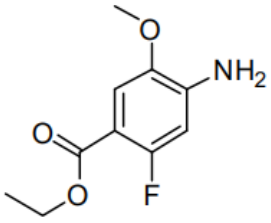

Obtained using procedure H on 9.1 mmol scale; 1.92 g, 9.0 mmol, yield 98%, light orange solid. ^{1}H NMR (500 MHz, $CDCl_3$) δ 7.27 (d, *J* = 6.4 Hz, 1H), 6.37 (d, *J* = 11.9 Hz, 1H), 4.34 (q, *J* = 7.1 Hz, 4H), 3.86 (s, 3H), 1.37 (t, *J* = 7.1 Hz, 3H). ^{13}C NMR (126 MHz, $CDCl_3$) δ 164.90 (d, *J* = 4.3 Hz), 158.4, (d, *J* = 252.8 Hz), 142.4 (d, *J* = 12.1 Hz), 142.25 (d, *J* = 1.4 Hz), 111.92 (d, *J* = 2.8 Hz), 106.0 (d, *J* = 10.8 Hz), 101.4 (d, *J* = 28.4 Hz), 60.65, 55.95, 14.38.

ethyl 4-amino-2-fluoro-5-methoxybenzoate (15)

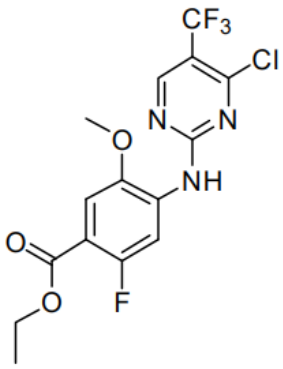

Obtained using procedure I on 9.0 mmol scale; 1.4 g, 3.6 mmol, yield 40%, offwhite solid. ^{1}H NMR (500 MHz, $CDCl_3$) δ 8.66 (s, 1H), 8.40 (d, *J* = 12.9 Hz, 1H), 8.29 (s, 1H), 7.40 (d, *J* = 6.3 Hz, 1H), 4.39 (q, *J* = 7.1 Hz, 2H), 3.95 (s, 3H), 1.40 (t, *J* = 7.1 Hz, 3H). ^{13}C NMR (126 MHz, $CDCl_3$) δ 164.3 (d, *J* =4.3 Hz), 159.6, 159.4, 157.3 (q, *J* = 4.9 Hz), 157.0 (d, *J* = 252.8 Hz), 143.4, 132.5 (d, *J* = 12.2 Hz), 122.3 (q, *J* = 272.2 Hz),111.7, 115.1 (d, *J* = 34.2 Hz), 111.6 (d, *J* = 1.6 Hz), 107.3 (d, *J* = 32.1 Hz), 99.8, 61.3, 56.4, 14.3. HRMS (ESI): m/z calcd for $C_{15}H_{13}O_3N_3ClF_4$ $[M+H]^+$:394.0576; found 394.0572.

ethyl 4-amino-2-fluoro-5-methoxybenzoate (16)

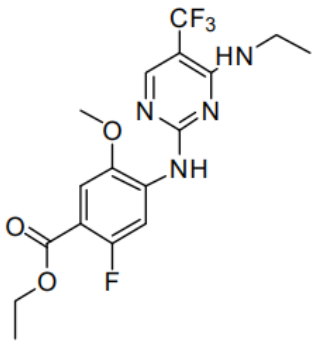

Obtained using procedure J on 3.3 mmol scale; 1.2 g, 2.9 mmol, yield 88%, offwhite solid. ^{1}H NMR (500 MHz, $CDCl_3$) δ 8.48 (d, *J* = 13.7 Hz, 1H), 8.19 (s, 1H), 7.93 (s, 1H), 7.37 (d, *J* = 6.4 Hz, 1H), 5.24 (s, 1H), 4.38 (q, *J* = 7.1 Hz, 2H), 3.94 (s, 3H), 3.63 - 3.59 (m, 2H), 1.40 (t, *J* = 7.1 Hz, 3H), 1.33 (t, *J* = 7.2 Hz, 3H).^{13}C NMR (126 MHz, $CDCl_3$) δ 164.6 (d, *J* = 4.3 Hz), 160.2, 158.9, 157.3 (d, *J* = 251.5 Hz), 154.6 (q, *J* = 5.3 Hz), 143.1, 134.4 (d, *J* = 12.9 Hz), 124.7 (q, *J* = 270.4 Hz), 111.2, 109.7 (d, *J* = 11.6 Hz), 106.4 (d, *J* = 32.6 Hz), 99.8, 61.1, 56.3, 36.5, 14.4, 14.3. HRMS (ESI): m/z calcd for $C_{17}H_{19}O_3N_4F_4$ $[M+H]^+$:403.1388; found 403.1385.

4-((4-(ethylamino)-5-(trifluoromethyl)pyrimidin-2-yl)amino)-2-fluoro-5-methoxybenzoic acid (17)

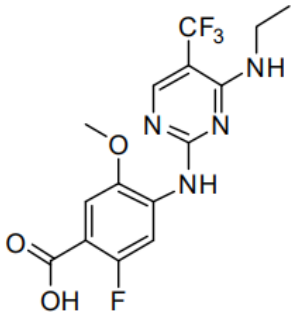

Obtained using procedure E on 1.85 mmol scale; 670 mg, 1.8 mmol, yield 97%, yellow solid. ^{1}H NMR (500 MHz, DMSO-*d*6) δ 12.93 (s, 1H), 8.35 (d, *J* = 13.7 Hz, 1H), 8.26 (s, 1H), 8.16 (s, 1H), 7.46 (t, *J* = 5.3 Hz, 1H), 7.36 (d, *J* = 6.7 Hz, 1H), 3.91 (s, 3H), 3.50 – 3.47 (m, 2H), 1.17 (t, *J* = 7.1 Hz, 3H). ^{13}C NMR (126 MHz, DMSO-*d*6) δ 164.8 (d, *J* = 3.5 Hz), 160.0, 157.8, 156.2 (d, *J* = 250.0 Hz), 154.6, 143.5, 133.8 (d, *J* = 12.5 Hz), 124.6 (q, *J* = 270.3 Hz), 111.8, 110.3 (d, *J* = 11.5 Hz), 106.4 (d, *J* = 23.2 Hz), 99.5 (d, *J* = 32.0 Hz), 56.4, 35.7, 14.2. HRMS (ESI): m/z calcd for $C_{15}H_{15}O_3N_4F_4$ $[M+H]^+$:375.1075; found 375.1071.

***tert*-butyl((4-(4-((4-(ethylamino)-5-(trifluoromethyl)pyrimidin-2-yl)amino)-2-fluoro-5-methoxybenzoyl)morpholin-2-yl)methyl)carbamate (18)**

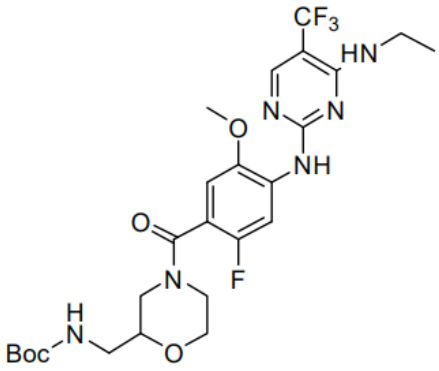

Obtained using procedure Q2 on 0.26 mmol scale; 55 mg, 0.11 mmol, yield 40%, yellow oil. ^{1}H NMR (500 MHz, $CDCl_3$) δ 8.42 (t, *J* = 11.1 Hz, 1H), 8.18 (s, 1H), 7.90 (s, 1H), 6.88 (s, 1H), 5.24 (s, 1H), 4.91 (s, 1H), 4.56 (t, *J* = 14.4 Hz, 1H), 3.91 (s, 3H), 3.60 – 3.49 (m, 6H), 3.37 – 3.21 (m, 2H), 3.03 – 2.94 (m, 2H), 1.38 (s, 9H), 1.31 (b, 3H).^{13}C NMR (126 MHz, $CDCl_3$) δ 165.6 (d, *J* = 12.7 Hz), 160.2, 158.8, 155.8, 154.4 (q, *J* = 4.9 Hz), 152.2 (d, *J* = 239.0 Hz), 144.2, 132.0 (d, *J* = 12.9 Hz), 124.7 (q, *J* = 269.7 Hz), 114.0, 109.7, 105.6 (d, *J* = 30.4 Hz), 99.8, 79.5, 74.9, 66.6, 56.2, 47.1, 42.4, 42.1, 36.429.6, 28.3, 28.2, 14.4. HRMS (ESI): m/z calcd for $C_{25}H_{33}O_5N_6F_4$ $[M+H]^+$: 573.2443; found 573.244.

2-(2,6-dioxopiperidin-3-yl)-4-nitroisoindoline-1,3-dione (19)

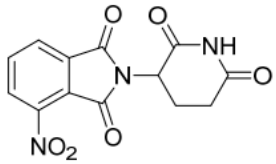

Obtained using procedure K on 10 mmol scale; 2.7 g, 8.9 mmol, yield 90%, purple solid. The crude product was used directly in the next step.^{1}H NMR (500 MHz, DMSO-*d*6) δ 11.20 (s, 1H), 8.36 (dd, *J* = 8.1, 0.7 Hz, 1H), 8.25 (dd, *J* = 7.5, 0.5 Hz, 1H), 8.14 – 8.11 (m, 1H), 5.21 (dd, *J* = 12.9, 5.4 Hz, 1H), 2.90 (ddd, *J* = 17.3, 14.0, 5.4 Hz, 1H), 2.64 – 2.61 (m, 1H), 2.56– 2.52 (m, 1H), 2.11 -2.06 (m, 1H).^{13}C NMR (126 MHz, DMSO-*d*6) δ 172.8, 169.6, 165.3, 162.6, 144.5, 136.9, 133.1, 129.0, 127.4, 122.6, 49.5, 30.9, 21.8.

4-amino-2-(2,6-dioxopiperidin-3-yl)isoindoline-1,3-dione (20)

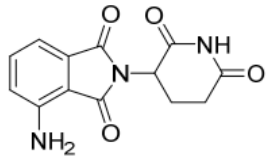

Obtained using procedure L on 8 mmol scale; 2.0 g, 7.3 mmol, yield 92%, yellowsolid. ^{1}H NMR (500 MHz, DMSO-*d*6) δ 11.09 (s, 1H), 7.46 (dd, *J* = 8.4, 7.0 Hz, 1H), 7.02 – 6.99 (m, 2H), 6.52 (b, 2H), 5.04 (dd, *J* = 12.7, 5.4 Hz, 1H), 2.88 (ddd, *J* = 17.0, 13.9, 5.5 Hz, 1H), 2.54 – 2.50 (m, 1H), 2.04 – 2.00 (m, 1H).^{13}C NMR (126 MHz, DMSO-*d*6) δ 172.9, 170.2, 168.6, 167.4, 146.8, 135.5, 132.0, 121.7, 111.0, 108.5, 48.5, 31.01, 22.2.

5-((2-(2,6-dioxopiperidin-3-yl)-1,3-dioxoisoindolin-4-yl)amino)-5-oxopentanoic acid (21)

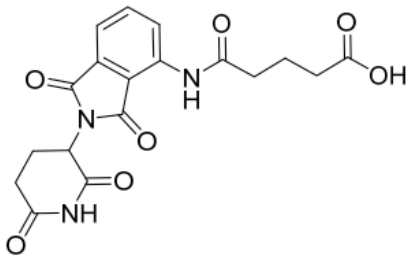

Obtained using procedure M on 7.3mmol scale; 904 mg, 2.4 mmol, yield 32%, white solid. ^{1}H NMR (500 MHz, DMSO-*d*6) δ 11.14 (s, 1H), 9.73 (s, 1H), 8.43 (d, *J* = 8.3 Hz, 1H), 7.84 – 7.81 (m, 1H), 7.61 (d, *J* = 7.3 Hz, 1H), 5.14 (dd, *J* = 12.9, 5.4 Hz, 1H), 2.92 – 2.85 (m, 1H), 2.62 – 2.50 (m, 4H), 2.30 (t, *J* = 7.3 Hz, 2H), 2.08 – 2.05 (m, 1H), 1.86 – 1.80 (m, 2H).^{13}C NMR (126 MHz, DMSO-*d*6) δ 174.0, 172.7, 171.5, 169.7, 167.5, 166.6, 136.3, 136.0, 131.4, 126.5, 118.3, 117.2, 48.8, 35.5, 32.7, 30.7, 21.9, 20.1. HRMS (ESI): m/z calcd for $C_{18}H_{18}O_7N_3$ $[M+H]^+$:388.1139; found 388.114.

2-chloro-N-(2-(2,6-dioxopiperidin-3-yl)-1,3-dioxoisoindolin-4-yl)acetamide (22)

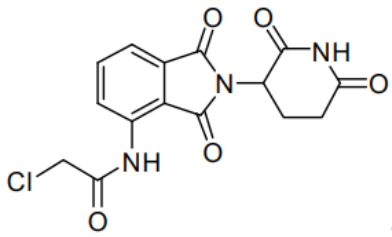

Obtained using procedure N on 5 mmol scale; 1.61 g, 4.6 mmol, yield 92%, yellow solid. ^{1}H NMR (500 MHz, DMSO-*d*6) δ 11.03 (s, 1H), 10.20 (s,1H), 7.81 (d, *J* = 7.6 Hz, 1H), 7.57 – 7.51 (m, 2H), 5.16 (dd, *J* = 13.3, 5.1 Hz, 1H), 4.32 (s, 2H), 2.95 – 2.88 (m, 1H), 2.62 – 2.59 (m, 1H), 2.34 (dd, *J* = 13.1, 4.4 Hz, 1H), 2.04 – 2.00 (m, 1H).^{13}C NMR (126 MHz, DMSO-*d*6) δ 172.8, 171.1, 167.7, 165.0, 134.1, 132.9, 132.8, 128.8, 125.6, 125.4, 119.8, 51.5, 43.1, 31.2, 22.6.

***tert*-butyl((1-(2-((2-(2,6-dioxopiperidin-3-yl)-1,3-dioxoisoindolin-4-yl)amino)-2-oxoethyl) piperidin- 4-yl)methyl)carbamate (23)**

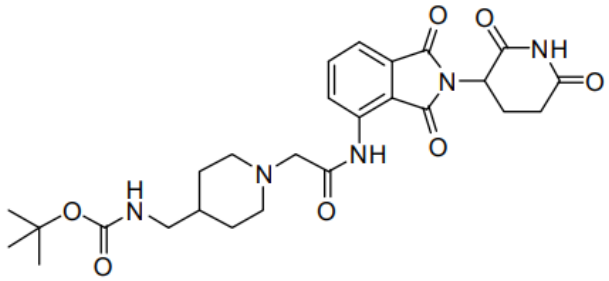

Obtained using procedure O on 3.44 mmol scale; 1.47 g, 2.8 mmol, yield 81%, light yellow solid. ^{1}H NMR (500 MHz, DMSO-*d*6) δ 11.14 (s, 1H), 11.02 (s, 1H), 8.79 (d, *J* = 8.5 Hz, 1H), 7.84 (t, *J* = 7.9 Hz, 1H), 7.58 (d, *J* = 7.3 Hz, 1H), 6.88 (t, *J* = 5.7 Hz, 1H), 5.16 (dd, *J* = 12.9, 5.3 Hz, 1H), 4.10 (q, *J* = 5.2 Hz, 2H), 3.17 (d, *J* = 5.2 Hz, 6H), 2.87 – 2.82 (m, 3H), 2.63 – 2.54 (m, 2H), 2.21 – 2.07 (m, 2H), 1.65 – 1.63 (m, 2H), 1.37 (s, 9H).^{13}C NMR (126 MHz, DMSO-*d*6) δ 172.8, 170.5, 169.9, 168.0, 166.8, 163.2, 159.8, 155.7, 136.4, 131.4, 124.1, 117.9, 115.7, 77.4, 61.8, 53.3, 48.9, 45.5, 35.5, 30.9, 29.6, 28.3, 21.9. HRMS (ESI): m/z calcd for $C_{26}H_{34}O_7N_5$ $[M+H]^+$:528.2453; found 528.2448.

2-(2,6-dioxopiperidin-3-yl)-4-fluoroisoindoline-1,3-dione (24)

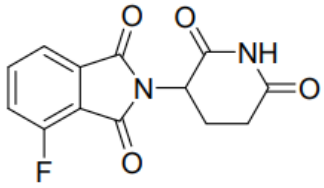

Obtained using procedure K on 5 mmol scale; 1.2 g, 4.3 mmol, yield 85%, white solid. The crude product was purified by column chromatography (DCM – MeOH, 0 – 5% MeOH in DCM). ^{1}H NMR (500 MHz, DMSO-*d*6) δ 11.16 (s, 1H), 7.96 – 7.92 (m, 1H), 7.79 (d, *J* = 7.3 Hz, 1H), 7.75 – 7.7.2 (m, 1H), 5.16 (dd, *J* = 13.0, 5.4 Hz, 1H), 2.91 – 2.85 (m, 1H), 2.63 – 2.58 (m, 1H), 2.53 – 2.51 (m, 1H), 2.07 – 2.04 (m, 1H). ^{13}C NMR (126 MHz, DMSO-*d*6) δ 172.8, 169.7, 166.1, 164.0, 156.8 (d, *J* = 262.3 Hz), 138.0 (d, *J* = 7.9 Hz), 133.5, 123.0 (d, *J* = 19.6 Hz), 120.1 (d, *J* = 3.2 Hz), 117.0 (d, *J* = 12.6 Hz), 49.1, 30.9, 21.9.

tert-butyl(3-((2-(2,6-dioxopiperidin-3-yl)-1,3-dioxoisoindolin-4-yl)amino)propyl) carbamate (25)

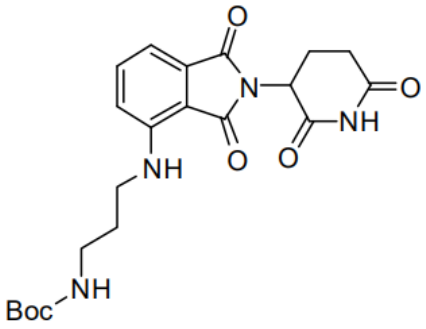

Obtained using procedure P on 1.03 mmol scale; 266 mg, 0.6 mmol, yield 60%, yellow solid. ^{1}H NMR (500 MHz, $CDCl_3$) δ 8.09 (s, 1H), 7.51 – 7.48 (m, 1H), 7.10 (d, *J* = 7.1 Hz, 1H), 6.88 (d, *J* = 8.5 Hz, 1H), 6.31 (s, 1H), 4.91 (dd, *J* = 12.4, 5.3 Hz, 1H), 4.65 (s, 1H), 3.35 – 3.31 (m, 2H), 3.26 – 3.25 (m, 2H), 2.82 – 2.72 (m, 3H), 2.14 – 2.10 (m, 1H), 1.87 – 1.83 (m, 2H), 1.44 (s, 9H).^{13}C NMR (126 MHz, $CDCl_3$) δ 171.0, 169.4, 168.3, 167.6, 156.1, 146.7, 136.2, 132.5, 116.5, 111.6, 110.1, 79.5, 48.9, 43.4, 40.0, 31.4, 29.9, 28.4, 22.8.

tert-butyl(4-((2-(2,6-dioxopiperidin-3-yl)-1,3-dioxoisoindolin-4-yl)amino)butyl) carbamate (26)

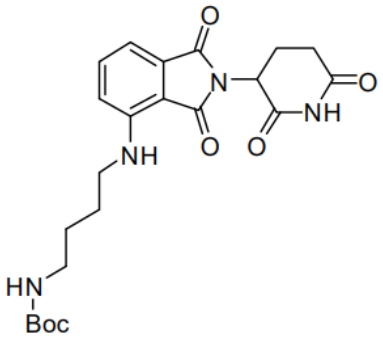

Obtained using procedure P on 1.03 mmol scale; 270 mg, 0.6 mmol, yield 60%, yellow solid. ^{1}H NMR (500 MHz, $CDCl_3$) δ 8.37 (s, 1H), 7.47 (dd, *J* = 8.3, 7.3 Hz, 1H), 7.08 (d, *J* = 7.1 Hz, 1H), 6.87 (d, *J* = 8.5 Hz, 1H), 6.23 (d, *J* = 5.6 Hz, 1H), 4.91 (dd, *J* = 12.3, 5.4 Hz, 1H), 4.62 (s, 1H), 3.31 – 3.27 (m, 2H), 3.18 – 3.16 (m, 2H), 2.86 – 2.72 (m, 3H), 2.13 – 2.10 (m, 1H), 1.70 – 1.67 (m, 2H), 1.65 – 1.57 (m, 2H), 1.43 (s, 9H).^{13}C NMR (126 MHz, $CDCl_3$) δ 171.2, 169.5, 168.4, 167.6, 156.0, 146.8, 136.1, 132.4, 116.6, 111.5, 109.9, 79.3, 48.8, 42.2, 31.4, 28.4, 27.5, 26.4, 22.8.

_N_1-((4-(5-(3-cyanophenyl)-7_H_-pyrrolo[2,3-d]pyrimidin-4-yl)morpholin-2-yl)methyl)-N5-(2-(2,6-dioxopiperidin-3-yl)-1,3-dioxoisoindolin-4-yl)glutaramide (27)

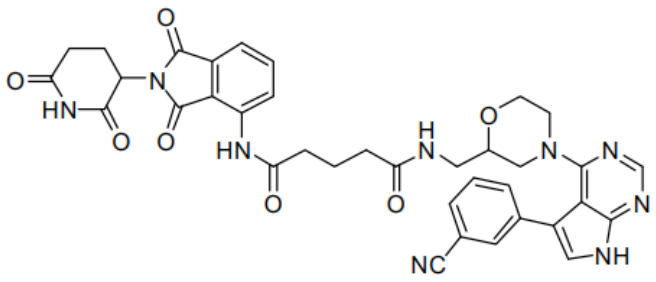

Obtained using procedure Q1 on 0.27 mmol scale; 75 mg, 0.11 mmol, yield 40%, yellow solid.^{1}H NMR (500 MHz, $CDCl_3$) δ 11.10 (s, 1H), 9.40 (s, 1H), 8.75 (d, *J* = 8.5 Hz, 1H), 8.46 (s, 1H), 7.77 – 7.75 (m, 1H), 7.71 (d, *J* = 7.8 Hz, 1H), 7.69 – 7.65 (m, 1H), 7.60 – 7.58 (m, 1H), 7.52 (dd, *J* = 9.9, 7.6 Hz, 2H), 6.07 – 6.05 (m, 1H), 4.97 (dd, *J* = 12.2, 5.4 Hz, 1H), 3.69 – 3.64 (m, 2H), 3.57 – 3.52 (m, 1H), 3.46 – 3.39 (m, 2H), 3.33 (dd, *J* = 8.9, 4.9 Hz, 1H), 3.00 – 2.97 (m, 1H), 2.90 – 2.85 (m, 2H), 2.80 – 2.76 (m, 2H), 2.65 – 2.63 (m, 1H), 2.52 (t, *J* = 7.2

Hz, 2H), 2.29 (t, *J* = 7.1 Hz, 2H), 2.15 – 2.13 (m, 1H), 2.07 – 2.03 (m, 2H), 1.87 – 1.85 (m, 2H).^{13}C NMR (126 MHz, $CDCl_3$) δ 172.1, 171.8, 169.0, 168.8, 166.7, 160.1, 153.3, 150.7, 137.6, 136.5, 136.3, 132.3, 131.6, 131.1, 130.1, 129.5, 125.3, 122.2, 118.7, 118.5, 115.4, 115.0, 112.6, 103.0, 76.8, 74.0, 66.0, 51.6, 49.3, 41.3, 36.6, 35.0, 31.4, 22.7, 21.0, 20.9. HRMS (ESI): m/z calcd for $C_{36}H_{34}O_7N_9$ $[M+H]^+$:704.2576; found 704.2571.

4-(5-(3-cyanophenyl)-7*H*-pyrrolo[2,3-d]pyrimidin-4-yl)-N-(3-((2-(2,6-dioxopiperidin-3-yl)-1,3-dioxoisoindolin-4-yl)amino)propyl)morpholine-2-carboxamide (28)

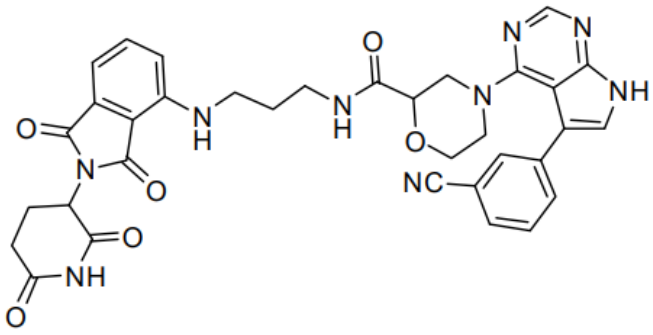

Obtained using procedure Q1 on 0.10 mmol scale; 35 mg, 0.05 mmol, yield 50%, white solid.^{1}H NMR (500 MHz, $CDCl_3$) δ 10.46 (s, 1H), 9.00 (s, 1H), 8.52 (s, 1H), 7.83 (s, 1H), 7.78 (d, *J* = 7.5 Hz, 1H), 7.60 – 7.54 (m, 2H), 7.51 – 7.48 (m, 1H), 7.10 (d, *J* = 7.1 Hz, 1H), 6.87 (d, *J* = 8.6 Hz, 1H), 6.62 (t, *J* = 5.3 Hz, 1H), 6.41 (t, *J* = 5.8 Hz, 1H), 4.96 – 4.93 (m, 1H), 4.06 (d, *J* = 11.5 Hz, 1H), 3.83 (d, *J* = 10.8 Hz, 2H), 3.70 (d, *J* = 12.7 Hz, 1H), 3.57 (t, *J* = 11.4 Hz, 1H), 3.35 (q, *J* = 6.5 Hz, 2H), 3.31 – 3.28 (m, 2H), 2.97 (t, *J* = 12.1 Hz, 1H), 2.90 – 2.86 (m, 1H), 2.83-2.74 (m, 2H), 2.71 – 2.66 (m, 2H), 2.14 – 2.11 (m, 1H), 1.84 – 1 .79 (m, 2H). ^{13}C NMR (126 MHz, $CDCl_3$) δ 171.5, 169.3, 169.1, 167.6, 160.0, 153.4, 146.6, 136.4, 136.1, 132.6, 132.4, 131.9, 130.1, 129.6, 127.5, 122.1, 118.8, 116.4, 115.3, 112.6, 111.6, 110.2, 88.8, 74.7, 66.0, 52.0, 48.9, 39.9, 36.2, 31.5, 30.9, 29.2, 22.8. HRMS (ESI): m/z calcd for $C_{34}H_{32}O_6N_9$ $[M+H]^+$:662.247; found 662.2467.

4-(5-(3-cyanophenyl)-7*H*-pyrrolo[2,3-d]pyrimidin-4-yl)-N-((1-(2-((2-(2,6-dioxopiperidin-3-yl)-1,3-dioxoisoindolin-4-yl)amino)-2-oxoethyl)piperidin-4-yl)methyl)morpholine-2-arboxamide (29)

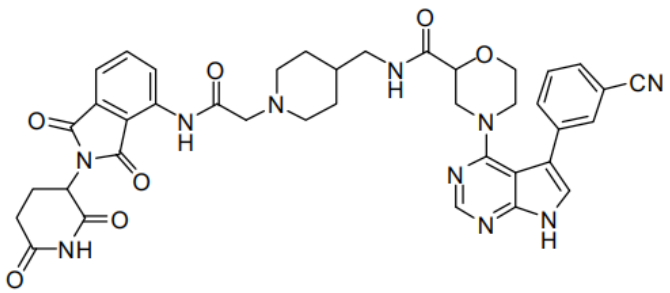

Obtained using procedure Q1 on 0.10 mmol scale; 30 mg, 0.04 mmol, yield 40%, yellow solid.^{1}H NMR (500 MHz, $CDCl_3$) δ 11.39 (s, 1H), 10.95 (s, 1H), 8.85 – 8.81 (m, 1H), 8.50 (d, *J* = 10.7 Hz, 1H), 7.81 (d, *J* = 6.0 Hz, 1H), 7.73 – 7.68 (m, 2H), 7.59 – 7.53 (m, 3H), 6.48 – 6.47 (m, 1H), 5.04 – 4.99 (m, 1H), 3.99 (d, *J* = 12.7 Hz, 1H), 3.87 (d, *J* = 11.0 Hz, 1H), 3.80 – 3.74 (m, 2H), 3.62 – 3.59 (m, 1H), 3.31 – 3.21 (m, 2H), 3.18 – 3.02 (m, 3H), 2.95 – 2.86 (m, 4H), 2.81 – 2.77 (m, 1H), 2.64 – 2.61 (m, 1H), 2.34 – 2.30 (m, 1H), 2.23 – 2.20 (m, 2H), 2.01 – 2.00 (b, 1H), 1.80 – 1.78 (m, 1H), 1.71 – 1.62 (m, 3H), 1.47 – 1.42 (m, 2H).^{13}C NMR (126 MHz, $CDCl_3$) δ 172.0, 170.9, 168.6, 168.2, 166.9, 160.1, 153.4, 150.7, 137.0, 136.1, 132.8, 131.5, 130.1, 129.5, 124.7, 122.3, 119.0, 118.3, 116.0, 115.2, 112.6, 103.3, 74.8, 66.0, 62.1, 53.8, 52.4, 49.2, 48.2, 44.2, 35.2, 31.2, 30.0, 23.1. HRMS (ESI): m/z calcd for $C_{39}H_{39}O_7N_{10}$ $[M+H]^+$:759.2998; found 759.3002.

5-(4-(5-(3-cyanophenyl)-7H-pyrrolo[2,3-d]pyrimidin-4-yl)piperazin-1-yl)-N-(2-(2,6-dioxopiperidin-3-yl)-1,3-dioxoisoindolin-4-yl)-5-oxopentanamide (30)

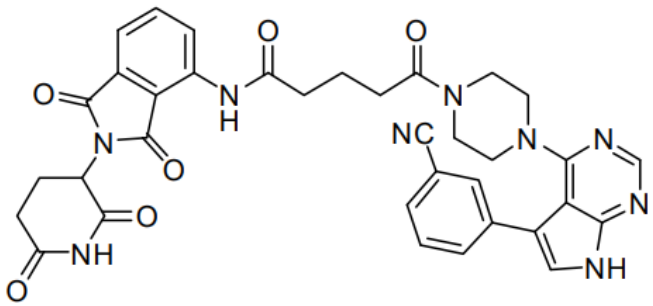

Obtained using procedure Q1 on 0.12 mmol scale; 40 mg, 0.06 mmol, yield 50%, off-white solid.^{1}H NMR (500 MHz, $CDCl_3$) δ 11.29 (s, 1H), 10.05 (s, 1H), 9.39 (s, 1H), 8.77 (d, *J* = 8.5 Hz, 1H), 7.80 (s, 1H), 7.75 – 7.68 (m, 2H), 7.59 (d, *J* = 7.7 Hz, 1H), 7.54 – 7.52 (m, 2H), 7.28 (s, 1H), 4.96 (dd, *J* = 12.3, 5.3 Hz, 1H), 3.41 – 3.37 (m, 6H), 3.18 (b, 2H), 2.93 – 2.90 (m, 1H), 2.82 – 2.77 (m, 2H), 2.55 (dd, *J* = 6.8, 5.3 Hz, 2H), 2.42 (t, *J* = 7.1 Hz, 2H), 2.16 – 2.10 (m, 1H), 2.08 – 2.00 (m, 3H).^{13}C NMR (126 MHz, $CDCl_3$) δ 171.8, 171.7, 170.4, 169.0, 168.7, 166.7, 160.0, 153.3, 150.5, 137.6, 136.5, 136.4, 132.4, 131.7, 131.1, 130.1, 129.5, 125.3, 122.3, 118.6, 118.5, 115.4, 115.1, 112.7, 49.3, 48.7, 44.7, 40.8, 36.8, 31.9, 31.4, 29.7, 22.7, 20.4. HRMS (ESI): m/z calcd for $C_{35}H_{32}O_6N_9$ $[M+H]^+$:674.247; found 674.2466.

N^1-(2-(2,6-dioxopiperidin-3-yl)-1,3-dioxoisoindolin-4-yl)-N5-((4-(4-((4-(ethylamino)-5-(trifluoromethyl)pyrimidin-2-yl)amino)-2-fluoro-5-methoxybenzoyl)morpholin-2-yl)methyl)glutaramide (31)

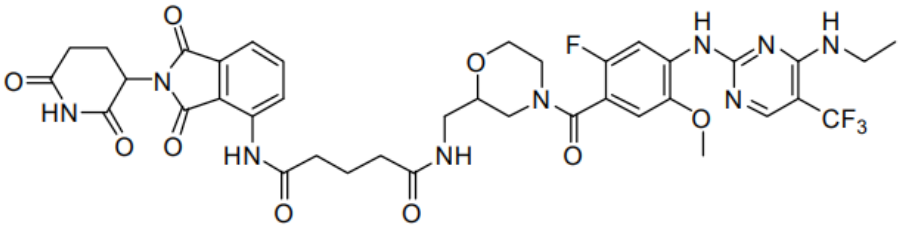

Obtained using procedure Q1 on 0.11 mmol scale; 32 mg, 0.04 mmol, yield 35%, white solid.^{1}H NMR (500 MHz, $CDCl_3$) δ 9.42 (b, 1H), 8.78 (t, *J* = 7.3 Hz, 1H), 8.43 (dd, *J* = 12.1, 8.6 Hz, 1H), 8.19 (s, 1H), 7.89 – 7.85 (m, 1H), 7.70 (t, *J* = 7.9 Hz, 1H), 7.55 (d, *J* = 7.3 Hz, 1H), 6.90 (d, *J* = 5.7 Hz, 1H), 6.03 (s, 1H), 5.21 (s, 1H), 4.96 – 4.94 (m, 1H), 4.59 – 4.56 (m, 1H), 3.90 (s, 3H), 3.62 – 3.57 (m, 4H), 3.56 – 3.50 (m, 3H), 3.32 – 3.30 (m, 1H), 3.01 – 2.99 (m, 1H), 2.90 (dd, *J* = 12.9, 2.4 Hz, 1H), 2.76 (d, *J* = 11.3 Hz, 3H), 2.58 – 2.48 (m, 2H), 2.34 – 2.28 (m, 2H), 2.17 – 2.03 (m, 4H), 1.32 (t, *J* = 7.2 Hz, 3H).^{13}C NMR (126 MHz, $CDCl_3$) δ 172.1, 171.6, 170.9, 169.0, 168.0, 166.6, 165.7, 160.2, 158.8, 154.5, 152.2 (d, *J* = 238.5 Hz), 151.9, 144.3, 137.6, 136.4, 132.01, 131.1, 124.4 (d, *J* = 270 Hz) 118.6, 115.4, 109.8 (d, *J* = 4.6 Hz), 105.6, 99.9, 74.6, 66.6, 56.3, 49.3, 44.8, 42.2, 41.1, 36.4, 35.1, 31.3, 22.7, 21.0, 14.4. HRMS (ESI): m/z calcd for $C_{38}H_{40}O_9N_9F_4$ $[M+H]^+$:842.288; found 842.2875.

N-((1-(2-((2-(2,6-dioxopiperidin-3-yl)-1,3-dioxoisoindolin-4-yl)amino)-2-oxoethyl) piperidin-4-yl)methyl)-4-((4-(ethylamino)-5-(trifluoromethyl)pyrimidin-2-yl)amino)-2-fluoro-5-methoxybenzamide (32)

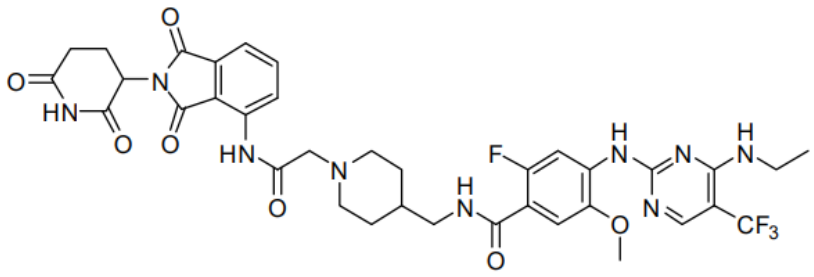

Obtained using procedure Q1 on 0.2 mmol scale; 80 mg, 0.11 mmol, yield 52%, off-white solid.^{1}H NMR (500 MHz, $CDCl_3$) δ 11.31 (s, 1H), 8.85 (d, *J* = 8.4 Hz, 1H), 8.43 (d, *J* = 15.2 Hz, 1H), 8.19 (s, 1H), 7.98 (b, 1H), 7.70 – 7.66 (m, 1H), 7.54 (dd, *J* = 20.0, 7.2 Hz, 2H), 6.86 (dt, *J* = 11.7, 5.6 Hz, 1H), 5.27 (b, 1H), 4.94 (dd, *J* = 11.9, 5.6 Hz, 1H), 3.93 (s, 3H), 3.61 – 3.58 (m, 2H), 3.50 – 3.46 (m, 1H), 3.40 – 3.47 (m, 1H), 3.21 – 3.12 (m, 2H), 2.95 – 2.92 (m, 2H), 2.89 – 2.86 (m, 2H), 2.78 – 2.74 (m, 2H), 2.33 (t, *J* = 10.1 Hz, 1H), 2.26 (t, *J* = 10.5 Hz, 1H), 2.18 – 2.15 (m, 1H), 1.78 – 1.76 (m, 2H), 1.65 – 1.63 (m, 3H), 1.30 (t, *J* = 7.2 Hz, 3H).^{13}C NMR (126 MHz, $CDCl_3$) δ 171.4, 170.9, 168.3, 168.0, 166.9, 163.5 (d, *J* = 3.8 Hz), 160.1, 158.7, 155.4 (d, *J* = 237.5 Hz), 144.0, 137.0, 136.1, 133.1 (d, *J* = 13.7 Hz), 131.4, 124.9, 124.6 (q, *J* = 267.9 Hz), 118.3, 116.0, 112.2 (d, *J* = 13.1 Hz), 111.2 (d, *J* = 3.3 Hz), 105.5 (d, *J* = 35.8 Hz), 99.8 (q, *J* = 32.3 Hz), 62.2, 56.3, 53.9, 49.2, 45.5, 36.4, 35.42, 31.3, 30.0, 29.75, 22.9, 14.4. HRMS (ESI): m/z calcd for $C_{36}H_{38}O_7N_9F_4$ $[M+H]^+$: 784.2825; found 784.282.

_N_-(4-((2-(2,6-dioxopiperidin-3-yl)-1,3-dioxoisoindolin-4-yl)amino)butyl)-4-((4-(ethylamino)-5-(trifluoromethyl)pyrimidin-2-yl)amino)-2-fluoro-5-methoxybenzamide (33)

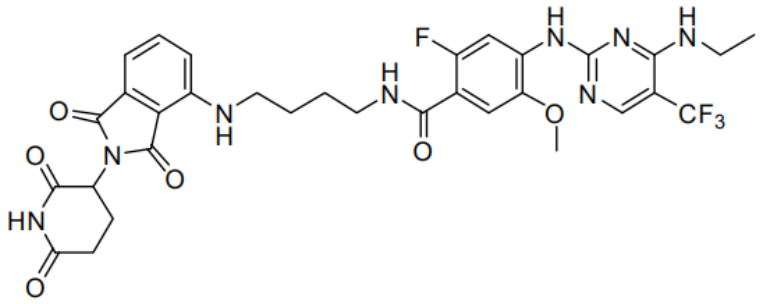

Obtained using procedure Q1 on 0.16 mmol scale; 58 mg, 0.08 mmol, yield 52%, yellow solid.^{1}H NMR (500 MHz, $CDCl_3$) δ 8.69 (s, 1H), 8.45 (d, *J* = 15.2 Hz, 1H), 8.20 (s, 1H), 7.97 (s, 1H), 7.55 (d, *J* = 7.1 Hz, 1H), 7.47 – 7.44 (m, 1H), 7.06 (d, *J* = 7.1 Hz, 1H), 6.88 (d, *J* = 8.5 Hz, 2H), 6.25 (t, *J* = 5.7 Hz, 1H), 5.26 (b, 1H), 4.91 (dd, *J* = 12.3, 5.3 Hz, 1H), 3.93 (s, 3H), 3.62 – 3.57 (m, 2H), 3.54 – 3.52 (m, 2H), 3.32 (d, *J* = 5.8 Hz, 2H), 2.88 – 2.80 (m, 1H), 2.77 – 2.69 (m, 2H), 2.13 – 2.09 (m, 1H), 1.76 – 1.74 (m, 4H), 1.32 (t, *J* = 7.2 Hz, 3H). ^{13}C NMR (126 MHz, $CDCl_3$) δ 171.3, 169.5, 168.6, 167.6, 163.5 (d, *J* = 3.8 Hz), 160.2, 158.8, 155.5 (d, *J* = 237.4 Hz), 146.8, 144.0, 136.1, 133.2 (d, *J* = 13.9 Hz), 132.5, 124.7 (q, *J* = 270.4 Hz), 116.7, 112.2 (d, *J* = 13.1 Hz), 111.5, 111.1 (d, *J* = 3.5 Hz), 110.0, 105.6 (d, *J* = 35.3 Hz), 99.9 (q, *J* = 33.2 Hz), 56.3, 48.9, 42.2, 39.5, 36.4, 31.4, 27.1, 26.7, 22.8, 14.4. HRMS (ESI): m/z calcd for $C_{32}H_{33}O_6N_8F_4$ $[M+H]^+$:701.2454; found 701.2451.

- **Biological screening**

1. Kinase assays

a. *In-vitro radioactive kinase assay*

LRRK2 kinase activity was measured using the previously described radiometric based LRRKtide assay.[s4, s5] Shortly, the reaction mixture consist of 0.1μM of purified full-length Strep flag LRRK2, 75μM LRRKtide (SignalChem, Cat No. L10-58), 25μM ATP (2 Ci/mmol, hot ATP from Perkin Elmer, Cat No.: BLU502Z250UC), kinase buffer (25mM Tris (pH 7.5), 15mM MgCl2, 20mM β-Glycerol phosphate, 1mM NaF, 1mM EGTA, 1mM Na3VO4, 2mM DTT) and the indicated concentrations of PROTACs or DMSO as control. The reaction was started by adding 75 μM (2 Ci/mmol) ATP-γ-32P and the mixture was incubated at 30°C. Samples were taken after 30 seconds and 30 minutes and spotted on nitrocellulose filters, washed with 75 mM phosphoric acid and dried before scintillation counting (Perkin Elmer).

b. *In-vitro kinase assay (Western Blot)*

The assay was performed for four different concentrations (1nM, 10nM, 0.1μM and 1μM) of PROTACs and their parent kinase inhibitor. The reaction mixture for every concentration included the solvent (DMSO) and consists of 100μM GDP, 25μM ATP, kinase buffer (containing 25mM Tris (pH 7.5), 15mM MgCl2, 20mM β-Glycerol phosphate, 1mM NaF, 1mM EGTA, 1mM Na3VO4, and 2mM DTT), and the indicated concentration of PROTACs (DMSO as control). The reaction was started by the addition of 0.1μM of purified full-length Strep flag LRRK2 and the mixture was incubated at 30° C. Samples were taken after 30 seconds and 30 minutes and immediately mixed with 4X Laemmli buffer and denatured at 95° C for 10 minutes. Auto-phosphorylation of LRRK2 was determined by western blotting using anti-phospho LRRK2 (phospho S1292) [MJFR-19-7-8] rabbit monoclonal antibody; 1:1000 dilution (Abcam, ab203181) and secondary goat anti-rabbit (HRP), 1:5000 dilution (Cell Signaling Technology®, #7074). Total LRRK2 was detected using anti-LRRK2 mouse monoclonal antibody; 1:1000 dilution (Biolegend®, AB_2750047 (BioLegend Cat. No. 844402)) and the secondary antibody anti-mouse m-IgGκ BP 1:5000 dilution (Santa Cruz Biotechnology®, sc-516142). Blots were visualized using LI-COR® WesternSure® PREMIUM Chemiluminescent Substrate with LI-COR C-DiGit® Blot Scanner (Model: 3600).

2. Cell culture

LRRK2 parental RAW 264.7 cells (ATCC® SC-6003™, passage number 3-13) were cultured in Dulbecco's Modified Eagle's medium (DMEM, ATCC® 30-2002™) supplemented with 10% FBS and 1% penicillin-streptomycin (Gibco™, 15070063). HEK293 cells were grown in Dulbecco's Modified Eagle's medium (DMEM, Gibco™, 11960044) supplemented with 10% FBS and 1% penicillin-streptomycin-Glutamine (Gibco™, 10378016). The cells used for the experiments were mycoplasma free (tested with MycoAlertTM Plus Mycoplasma Detection Kit, Lonza # LT07-703).

3. Microscopy

HEK293 cells were seeded in 8-well ibidi slide (# 80824) coated with poly L-lysine (30,000 cells/well). The next day cells were transfected with GFP-tagged LRRK2 using jetPEI® (101-10N) (Polyplus) according to the manufacturer's protocol. After 24hours of transfection, 10μM of different PROTACs, original kinase inhibitors and DMSO as controls were incubated for 3h, and followed by live imaging. Data acquisition was done using a 63x/1.40 oil-immersion plan apochromat objective of a LSM800 Airyscan confocal laser scanning microscope (Carl Zeiss) and image analysis was done using ZEN 2.3 lite (Carl Zeiss).

4. Western blotting for endogenous LRRK2 expression

RAW 264.7 cells were seeded in 6-well plate (600,000 cells/well) overnight before treatment with PROTACs (10μM) along with the original kinase inhibitors (10μM) and DMSO as controls. 24 hours after incubation, cells were washed with 50 mM Tris; pH 7.5, 100 mM NaCl, 5 mM MgCl2, 5% Glycerol and lysed for 1hr at 4°C using lysis buffer (50 mM Tris; pH 7.5, 100 mM NaCl, 5 mM MgCl2, 5% Glycerol, 1% Triton X-100) containing protease inhibitor cocktail powder, P2714 (Sigma (P2714-1BTL)), β-glycerophosphate (20 mM), NaF (5 mM) and Na3VO4 (1 mM). The cell lysates were centrifuged at 13,000 g for 10 minutes and the total protein content of the supernatant was determined using Pierce™ BCA Protein Assay kit. Samples were mixed with 4X Laemmli buffer and denatured at 95oC for 10 minutes. 40 μg of total protein per sample was loaded on 8% polyacrylamide gels. Following SDS-PAGE, the proteins were transferred to nitrocellulose membrane, incubated overnight at 4°C with anti-LRRK2 24D8 rat monoclonal antibody; 1:1000 dilution (Provided by Dr. Gloeckner, DZNE Tübingen, Germany) or anti-GAPDH rabbit monoclonal antibody; 1:5000 dilution (Cell Signaling Technology®, 14C10 #2118). The secondary antibodies used were goat anti-rat (HRP) 1:5000 dilution (ab97057) or goat anti-rabbit (HRP) 1:5000 dilution (Cell Signaling Technology®, #7074). The proteins were detected using the LI-COR® WesternSure® PREMIUM Chemiluminescent Substrate with LI-COR C-DiGit® Blot Scanner (Model: 3600).

5. Ubiquitin assay

HEK293 cells were transfected with GFP-tagged LRRK2 using jetPEI® for 48 hours and then treated with 10 μM of compound **11** (original kinase inhibitor) and PROTAC **33** (PROTAC compound derived from compound **11**) and DMSO control for 24 hours with or without the addition of 5 μM MG132 (proteasome inhibitor). After treatment, cells were collected, washed with washing buffer and lysed with lysis buffer (10 mM Tris/Cl pH 7.5; 150 mM NaCl; 0.5 mM EDTA; 0.5% NP-40) containing P2714, β-glycerophosphate (10 mM), NaF (50 mM) and Na3VO4 (1 mM), sodium pyrophosphate (1mM), 0.1 μg/ml mycocystin-LR (Enzo Life Sciences, Switzerland) and 10 mM of NEM (ubiquitinase inhibitor, to preserve the ubiquitin signal) for 1 hour at 4oC. The cell lysates were centrifuged at 20,000 rcf for 10 minutes at 4° C and the total protein content of the clear supernatant was determined using Pierce™ BCA Protein Assay kit. Immunoprecipitation was performed using GFP-Trap®_Dynabeads

(ChromoTek, gtd-20) to pull down LRRK2 overnight at 4° C. Western blot was performed for both the input sample and the immunoprecipitated GFP-tagged LRRK2 using anti-ubiquitin P4D1 mouse monoclonal antibody 1: 500 dilution (Cell Signaling Technology®, #3936) and anti-GFP (Invitrogen, A-1122) 1:2000 dilution.

Acknowledgements

This research has been supported (to A.D.) through ITN "Accelerated Early stage drug dIScovery" (AEGIS, grant agreement no. 675555). Moreover, funding was received from the National Institutes of Health (2R01 GM097082-05), the European Lead Factory (IMI; grant agreement no. 115489), the Qatar National Research Foundation (NPRP6-065-3-012). and, COFUNDs ALERT (grant agreement no. 665250) and Prominent (grant agreement no. 754425) and KWF Kankerbestrijding grant (grant agreement no. 10504). A.M.D. is the recipient of a Stichting Parkinson Fonds (SPF) grant and a Rosalind Franklin Fellowship co-funded by the European Union and the University of Groningen. A.K. is holder of a TUBITAK 2232 scholarship and additional funding was received from The Michael J. Fox Foundation for Parkinson's Research.

Conflict of Interest

The authors declare no conflict of interest.

Supplementary material

Experimental details. General procedures, characterization data (^{1}H NMR, ^{13}C NMR), and biological screening (kinase assays, cell culture, microscopy, western blotting, ubiquitin assay) data are available at:

https://chemistry-europe.onlinelibrary.wiley.com/action/downloadSupplement? doi=10.1002%2Fcmdc.202000872&file=cmdc202000872-sup-0001-misc_information.pdf

SUPPLEMENTARY FIGURES

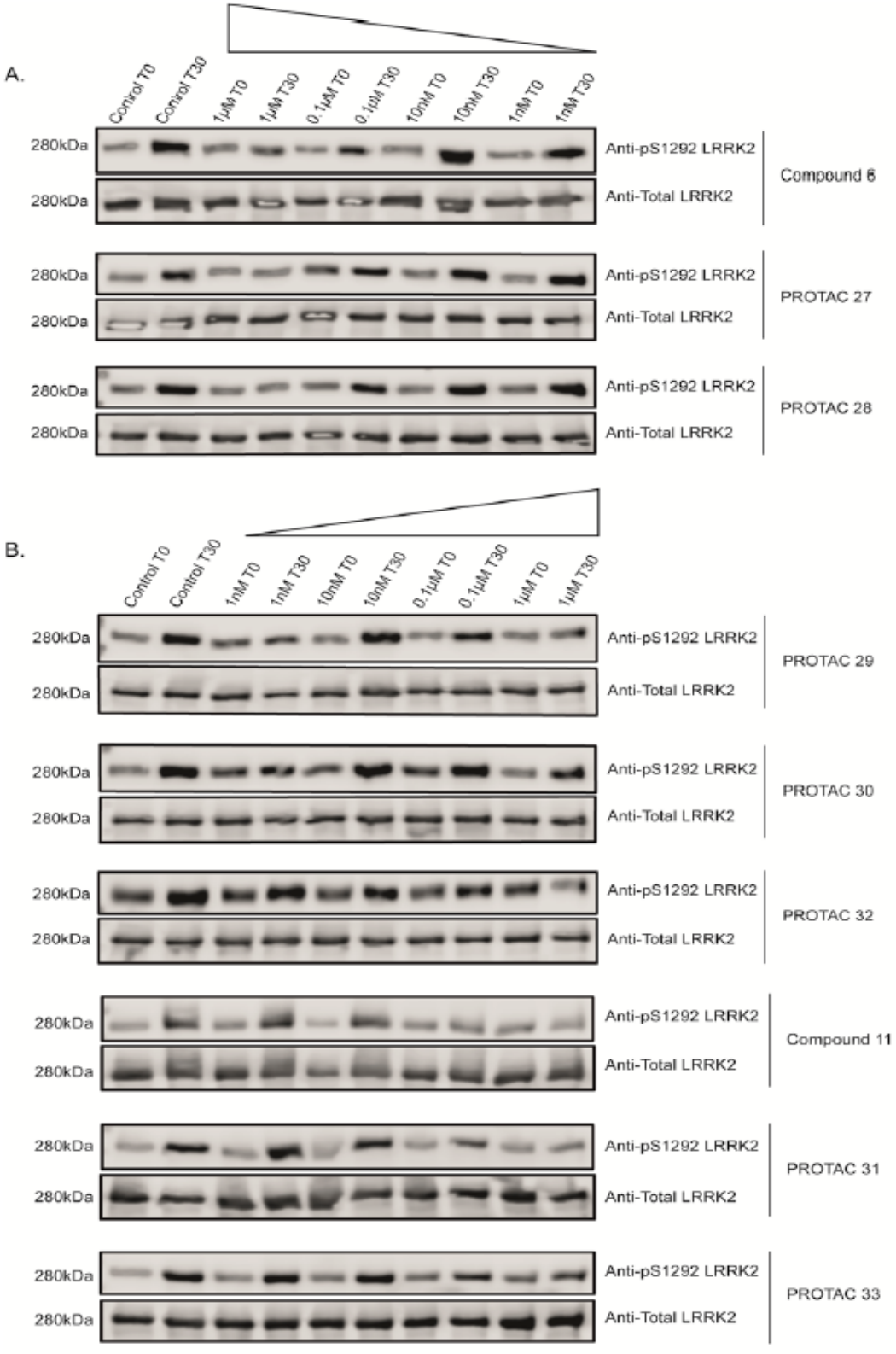

Figure S1. Western blot. PROTACs and their original kinase inhibitors inhibit LRRK2 kinase activity in a

concentration-dependent manner. A and B represents the pS1292 autophosphorylation of LRRK2 signal and total LRRK2 signal at T0 (0 minutes) and at T30 (30 minutes) for 1nM, 10nM, 0.1μM and 1μM concentrations of all PROTACs and their original kinase inhibitors.

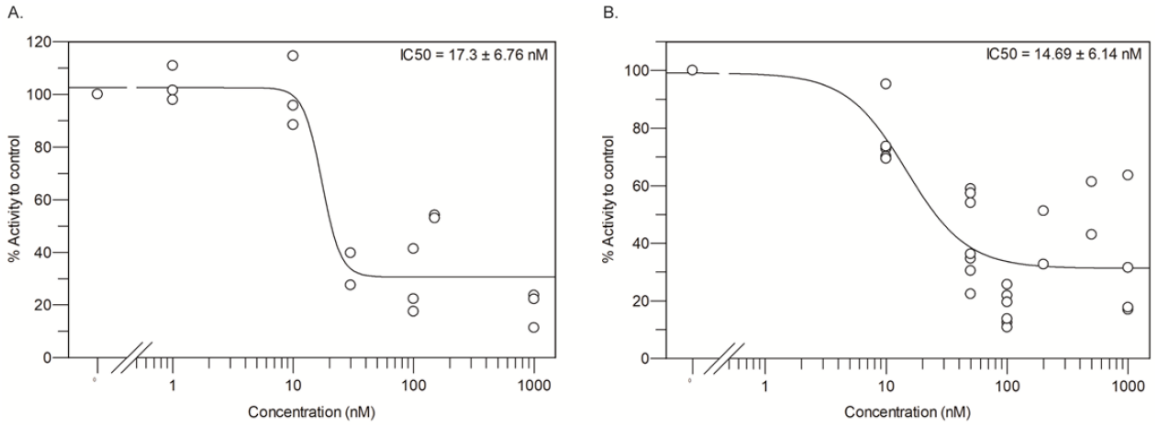

Figure S2. A and B represent the measurement of the kinase activity of LRRK2 (IC_{50}) at different concentrations of Compound (**11**) and PROTAC (**33**) respectively. The results are presented as percentage of kinase activity relative to the control.

REFERENCES

[1] W. P. Gilks, P. M. Abou-Sleiman, S. Gandhi, S. Jain, A. Singleton, A. J. Lees, K. Shaw, K. P. Bhatia, V. Bonifiati, N. P. Quinn, J. Lynch, D. G. Healy, J. L. Holton, T. Revesz, N. W. Wood, Lancet **2005**, 365, 415–416.

[2] S. Lesage, S. Janin, E. Lohmann, A. L. Leutenegger, L. Leclere, F. Viallet, P. Pollak, F. Durif, S. Thobois, V. Layet, M. Vidailhet, Y. Agid, A. Dürr, A. Brice, Arch. Neurol. **2007**, 64, 425–430.

[3] S. Bardien, S. Lesage, A. Brice, J. Carr, Parkinsonism Relat. Disord. 2011, 17, 501–508.

[4] R. Di Maio, E. K. Hoffman, E. M. Rocha, M. T. Keeney, L. H. Sanders, B. R. De Miranda, A. Zharikov, A. Van Laar, A. F. Stepan, T. A. Lanz, J. K. Kofler, E. A. Burton, D. R. Alessi, T. G. Hastings, J. T. Greenamyre, Sci. Transl. Med. **2018**, 10,eaar5429.

[5] B. I. Giasson, V. M. Van Deerlin, Neurosignals **2008**, 16, 99–105.

[6] D. J. Moore, Parkinsonism Relat. Disord. **2008**, 14 Suppl. 2, S92-S98.

[7] X. Deng, H. G. Choi, S. J. Buhrlage, N. S. Gray, Expert Opin. Ther. Pat. **2012**, 22, 1415–1426.

[8] R. R. Kethiri, R. Bakthavatchalam, Expert Opin. Ther. Pat. **2014**, 24, 745–757.

[9] P. Galatsis, Expert Opin. Ther. Pat. **2017**, 27, 667–676.

[10] https://clinicaltrials.gov/.

[11] J. L. Henderson, B. L. Kormos, M. M. Hayward, K. J. Coffman, J. Jasti, R. G. Kurumbail, T. T. Wager, P. R. Verhoest, G. S. Noell, Y. Chen, E. Needle, Z. Berger, S. J. Steyn, C. Houle, W. D. Hirst, P. Galatsis, J. Med. Chem. **2015**, 58, 419–432.

[12] A. A. Estrada, X. Liu, C. Baker-Glenn, A. Beresford, D. J. Burdick, M. Chambers, B. K. Chan, H. Chen, X. Ding, A. G. Di Pasquale, et al., J. Med. Chem. **2012**, 55, 9416–9433.

[13] https://www.proteinatlas.org/.

[14] P. Galatsis (Pfizer), US2017002000A1, **2017**.

[15] Y L. Chen (Novartis), WO2010015637A1, **2010**.

[16] J. C. Kath (Pfizer), WO2005023780A1,**2005**.

[17] N. Dzamko, M. Deak, F. Hentati, A. D. Reith, A. R. Prescott, D. R. Alessi, R. J. Nichols, Biochem. J. **2010**, 430,405–413.

[18] X. Deng, N. Dzamko, A. Prescott, P. Davies, Q. Liu, Q. Yang, J. D. Lee, M. P. Patricelli, T. K. Nomanbhoy, D. R. Alessi, N. S. Gray, Nat. Chem. Biol. **2011**, 7,203–205.

[19] M. B. Ramírez, A. J. Ordóñez, E. Fdez, J. Madero-Pérez, A. Gonnelli, M. Drouyer, M. C. Chartier-Harlin, J. M. Taymans, L. Bubacco, E. Greggio, S. Hilfiker, Hum. Mol. Genet. **2017**, 26,2747–2767.

[20] C. K. Deniston, J. Salogiannis, S. Mathea, D. M. Snead, I. Lahiri, M. Matyszewski, O. Donosa, R. Watanabe, J. Böhning, A. K. Shiau, S. Knapp, E. Villa, S. L. Reck-Peterson, A. E. Leschziner, Nature **2020**, 588, 344–349.

[21] R. Watanabe, R. L. Buschauer, J. Böhning, M. Audagnotto, K. Lasker, L. Tsan-Wen, D. Boassa,

S. Taylor, E. Villa, Cell **2020**, 182, 1508–1518.

[22] R. B. Kargbo, ACS Med. Chem. Lett. **2020**, 11, 2070–2071.

[23] N. S. Gray, J. Hatcher (Dana-Farber Cancer Institute), WO2020/081682 A, **2020**.

[24] A. W. Garofalo, J. Bright, S. De Lombaert, A. M. A. Toda, K. Zobel, D. Andreotti, C. Beato, S. Bernardi, F. Budassi, L. Caberlotto, et al., J. Med. Chem. **2020**, 63, 14821–14839.

SUPPLEMENTARY REFERENCES

[s1] J.L. Henderson, B.L. Kormos, M.M Hayward, K.J. Coffman, J. Jasti, R.G. Kurumbail, T.T. Wager, P.R. Verhoest, G.S. Noell, Y. Chen, E. Needle, Z. Berger, S.J. Steyn, C. Houle, W.D. Hirst, P. Galatsis, J. Med. Chem. **2015**, 58(1), 419-432.

[s2] Chen, Y-L. (Novartis), WO2010015637A1, **2010**.

[s3] A.A. Estrada, X. Liu, C. Baker-Glenn, A. Beresford, D.J. Burdick, M. Chambers, B.K. Chan, H. Chen, X. Ding, A.G. DiPasquale, S.L. Dominguez, J. Dotsonm, J. Drummond, M. Flagella, S. Flynn, R. Fuji, A. Gill, J. Gunzner-Toste, S.F. Harris, T.P. Heffron, T. Kleinheinz, D.W. Lee, C.E. Le Pichon, J.P. Lyssikatos, A.D. Medhurst, J.G. Moffat, S. Mukund, K. Nash, K. Scearce-Levie, Z. Sheng, D.G. Shore, T. Tran, N. Trivedi, S. Wang, S. Zhang, X. Zhang, G. Zhao, H. Zhu, Z.K. Sweeney. J. Med. Chem. **2012**, 55(22), 9416-9433.

[s4] G. Guaitoli, F. Raimondi, B.K. Gilsbach, Y. Gómez-Llorente, E. Deyaert, F. Renzi, X. Li, A. Schaffner, P.K.A. Jagtap, K. Boldt, F. Von Zweydorf, K. Gotthardt, D.D. Lorimer, Z. Yue, A. Burgin, N. Janjic, M. Sattler, W. Versées, M. Ueffing, I. Ubarretxena-Belandia, A. Kortholt, C.J. Gloeckner. s. Proc Natl Acad Sci. **2016**, 113(30), E4357-E4366.

[s5] B.K. Gilsbach, F.Y. Ho, I.R. Vetter, P.J.M. Van Haastert, A. Wittinghofer, A. Kortholt. Proc Natl Acad Sci. 2012, 109(26), 10322-10327.

AUTHOR CONTRIBUTION

Asmaa Oun, wrote the manuscript, and designed the tables, figures and the review layout. Angelica Maria Sabogal-Guaqueta participated in writing the microglia and intestinal organoid part. Sekar Galuh and Anastasia Alexander participated in writing the mitochondrial and the 3D model parts under the supervision of Arjan Kortholt and Amalia M. Dolga. All authors revised the manuscript before submission.